Science of the Total Environment 807 (2022) 150697

Contents lists available at ScienceDirect

Science of the Total Environment

journal homepage: www.elsevier.com/locate/scitotenv

Photo-enhanced toxicity of crude oil on early developmental stages of Atlantic cod (*Gadus morhua*)

Libe Aranguren-Abadía [a], Fekadu Yadetie [a], Carey E. Donald [c], Elin Sørhus [c], Lars Eirik Myklatun [a], Xiaokang Zhang [b], Kai K. Lie [c], Prescilla Perrichon [c], Charlotte L. Nakken [c], Caroline Durif [d], Steven Shema [e], Howard I. Browman [d], Anne Berit Skiftesvik [d], Anders Goksøyr [a], Sonnich Meier [c,1], Odd André Karlsen [a,1,*]

[a] Department of Biological Sciences, University of Bergen, Bergen, Norway
[b] Department of Molecular Oncology, Institute for Cancer Research, Oslo University Hospital-Radiumhospitalet, Oslo, Norway
[c] Institute of Marine Research, Bergen, Norway
[d] Institute of Marine Research, Austevoll Research Station, Storebø, Norway
[e] Grótti ehf., Grundarstíg 4, 101 Reykjavík, Iceland

HIGHLIGHTS

- UV radiation increased the toxicity of crude oil in early life stages of Atlantic cod.
- UV + oil increased larval malformations, including spinal curvature deformities.
- Photo-enhanced crude oil toxicity induced oxidative stress related gene pathways.
- UV + oil also affected pathways such as retinoid metabolism and circadian rhythms.

GRAPHICAL ABSTRACT

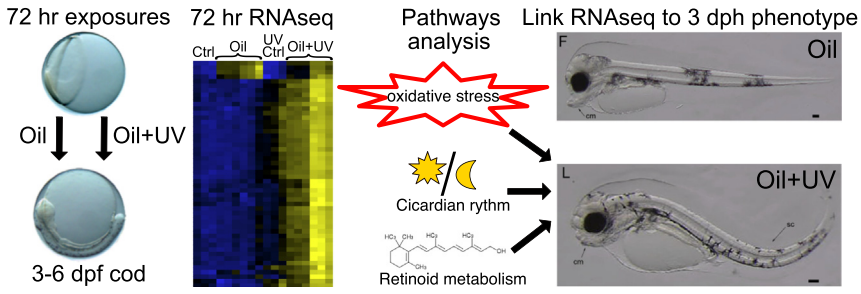

ARTICLE INFO

Article history:
Received 8 July 2021
Received in revised form 26 September 2021
Accepted 26 September 2021
Available online 2 October 2021

Editor: Jay Gan

Keywords:
Crude oil
UV-radiation
Photo-enhanced toxicity
Atlantic cod
Cyp1a

ABSTRACT

Photo-enhanced toxicity of crude oil is produced by exposure to ultraviolet (UV) radiation. Atlantic cod (*Gadus morhua*) embryos were exposed to crude oil with and without UV radiation (290–400 nm) from 3 days post fertilization (dpf) until 6 dpf. Embryos from the co-exposure experiment were continually exposed to UV radiation until hatching at 11 dpf. Differences in body burden levels and *cyp1a* expression in cod embryos were observed between the exposure regimes. High doses of crude oil produced increased mortality in cod co-exposed embryos, as well as craniofacial malformations and heart deformities in larvae from both experiments. A higher number of differentially expressed genes (DEGs) and pathways were revealed in the co-exposure experiment, indicating a photo-enhanced effect of crude oil toxicity. Our results provide mechanistic insights into crude oil and photo-enhanced crude oil toxicity, suggesting that UV radiation increases the toxicity of crude oil in early life stages of Atlantic cod.

© 2021 The Authors. Published by Elsevier B.V. This is an open access article under the CC BY license (http://creativecommons.org/licenses/by/4.0/).

1. Introduction

Exploration for petroleum resources off the coast of Lofoten, Vesterålen, and Senja in Northern Norway has been proposed by the

* Corresponding author.
E-mail address: odd.karlsen@uib.no (O.A. Karlsen).
[1] These authors share last authorship.

https://doi.org/10.1016/j.scitotenv.2021.150697
0048-9697/© 2021 The Authors. Published by Elsevier B.V. This is an open access article under the CC BY license (http://creativecommons.org/licenses/by/4.0/).

petroleum industry and the Norwegian government. These areas are crucial spawning and nursery grounds for important commercial fish species in the North Atlantic, including Northeast Arctic haddock (*Melanogrammus aeglefinus*), Northeast Atlantic cod (*Gadus morhua*), Northeast Arctic saithe (*Pollachius virens*) and Norwegian spring-spawning herring (*Clupea harengus*) (Olsen et al., 2009). Crude oil is a complex chemical mixture that contains thousands of different compounds, and large oil spills are toxic to marine life and have long-term effects on marine ecosystems (Barron et al., 2020). Petroleum exploration in this area is therefore controversial as it may pose a threat to numerous species at critical and sensitive developmental stages (Bjørkan and Veland, 2019; Misund and Olsen, 2013).

The early life stages (ELS) of fish are especially vulnerable to oil pollution and, in addition to acute mortality, numerous sublethal effects have been reported, including alterations in heart development, formation of heart and yolk sac edema, and craniofacial and spinal deformities (Carls et al., 1999; Cherr et al., 2017; Hodson, 2017; Incardona, 2017). Polycyclic aromatic hydrocarbons (PAHs) are considered the most bioavailable compounds present in the water soluble fraction (WSF) of crude oil and are therefore assumed to be the most toxic components of an oil spill (Carls and Meador, 2009; Carls et al., 1999). Certain PAHs are ligands for the ligand-activated transcription factor aryl hydrocarbon receptor (Ahr) (Denison and Nagy, 2003; Denison et al., 2011). The Ahr signaling pathway mediates responses to xenobiotics by regulating the transcription of enzymes involved in the biotransformation of exogenous compounds, including cytochrome P450 1A (Cyp1a) (Denison et al., 2011; Nebert, 2017; Okey, 2007; Whitlock, 1999). Induction of *cyp1a* is commonly used as a biomarker for exposure to PAHs and other environmental pollutants in fish (Celander, 2011; Goksøyr, 1995; Goksøyr and Förlin, 1992a; Nilsen et al., 1998; Schlenk et al., 2008; Stegeman and Hahn, 1994).

Exposure to sunlight, specifically ultraviolet (UV) radiation, increases the toxicity of petroleum more than 100-fold (Barron, 2017). Pelagic fish embryos and larvae are transparent and often found close to the water surface. It is therefore important to include photo-enhanced toxicity in risk management of potential oil spills when considering effects on pelagic fish embryos and larvae. Phototoxicity is linked to polyaromatic compounds, mainly 3–5 ring PAHs, as well as their oxygen, sulfur, and nitrogen analogs. These compounds absorb energy from UVB (280–320 nm) and UVA (320–400 nm) radiation, resulting in excited and reactive molecules (Arfsten et al., 1996; Barron, 2017). Photo-enhanced toxicity can be produced through two mechanisms: photomodification and photosensitization. Photomodification occurs when crude oil compounds are chemically modified via photooxidation. Photooxidation of crude oil in water may result in a chemical modification of compounds, which in some cases is more toxic (i.e. photomodification). Photosensitization occurs when bioaccumulated compounds cause tissue damage through photoexcitation within the animal, and it is believed to be the dominant mechanism in photo-enhanced toxicity in fish embryos and larvae (Barron, 2017). In photosensitization, bioaccumulated PAHs absorb UV, and when the energy from an excited state is transferred to oxygen molecules (photoexcitation) it can promote the formation of reactive oxygen species (ROS) and free radicals, leading to a state of oxidative stress (Barron, 2017; Roberts et al., 2017). Excess of ROS can lead to DNA damage, degradation of protein and lipids, mitochondrial dysfunction, alterations in Ca^{2+} homeostasis, and subsequent mitochondria-dependent apoptosis (Ermak and Davies, 2001; Görlach et al., 2015; Ott et al., 2007; Simon et al., 2000).

Atlantic cod (*Gadus morhua*) has been used as a bioindicator species in marine pollution monitoring programs and field studies, including monitoring of the water column in relation to offshore oil production in Norwegian waters (Beyer et al., 1996; Dale et al., 2019; Goksøyr et al., 1994; Husøy et al., 1996; Hylland et al., 2008; OSPAR, 2010; Sundt et al., 2012). Assessment of the effects of crude oil and oil related compounds on the ELS of Atlantic cod in the context of an oil spill has been a topic of interest (Goksøyr et al., 1991; Meier et al., 2010; Serigstad and Adoff, 1985; Sørensen et al., 2019, 2017; Tilseth et al., 1984). Atlantic cod eggs are translucent and float near the surface (Olsen et al., 2009), where they may be exposed to both crude oil and UV radiation during an oil spill. Extraction of crude-oil in spawning grounds of Atlantic cod and other fish increases the risk of ecological consequences in the event of an oil spill, and thus toxicological studies assessing the influence of phototoxicity are needed. The aim of this study was to assess phenotypic traits and molecular mechanisms involved in photo-enhanced toxicity of crude oil on the ELS of Atlantic cod by investigating morphological effects and transcriptomic changes in cod larvae and embryos, respectively, after embryonic exposure to crude oil with and without the presence of UV radiation.

2. Material and methods

2.1. Fish

Atlantic cod (*Gadus morhua*) were bred at the Institute of Marine Research (IMR) Austevoll Research Station. Fertilization of cod eggs was conducted in vitro using eggs and sperm stripped from three female fish and one male fish. Fertilized eggs were kept in egg incubators and maintained at 7 ± 1 °C until the crude oil exposure began.

2.2. Crude oil and UV light exposure

Exposure tanks were 50 L and made of green polyethylene plastic. Seawater flow was 32 L/h and the temperature of the seawater was maintained at 7 ± 1 °C. There were two parallel experiments: one with crude oil exposure without UV radiation, and another one with crude oil exposure combined with UV radiation. Exposure started at 3 days post fertilization (dpf) during the gastrulation and continued for 72 hours (h) until 6 dpf when the formation of the cardiac cone prior to the tubular heart begins (Hall et al., 2004) (for experimental design see Fig. S1). We selected this exposure window to match previous work (Sørhus et al., 2021). Cod have high background mortality during the transfer between maternal and zygotic transcription (from blastula to gastrula). We started exposures at 3 dpf to avoid including this high natural mortality in all treatments. Embryos were then transferred to new tanks with clean seawater. The UV radiation was continued in the recovery tanks until hatching at 11 dpf. All incubation tanks were illuminated using two broad spectrum 2 × 36 W Osram Biolux 965 (Munich, Germany, www.osram.com) dimmable fluorescent light tubes with 30 min smooth transitions between light and dark. The UV-exposed tanks had an additional two 40 W Q-Panel fluorescent bulbs (UVA-340 Q-Lab, Westlake, Ohio, USA; the UV irradiance is centered at 340 nm) suspended beneath the standard white light fluorescents. The Q-Panel lamps were aged for 100 h before the experiment began to ensure that they had reached a stable spectral output.

Incubation tanks were parallel to the axis of the fluorescent bulbs, resulting in slightly variable illumination between exposure tanks (Fig. S2). This was mitigated using a combination of black polyethylene sheets and aluminum foil, which shielded the non-UV-exposed tanks while reflecting and homogenizing the UV irradiance delivered to the UV-exposed tanks.

Irradiance was measured at several positions in each tank using an Ocean Optics Flame-S spectrometer. The optic fiber and Teflon cosine corrector were positioned vertically toward the light source 2–5 cm above the water's surface. The spectrometer measures photon flux at 0.5 nm intervals. These values were integrated across the relevant wavelength range (UV 280–400) to calculate the total spectral irradiance. To achieve the targeted daily doses, the UV bulbs were individually positioned to deliver the level of irradiance-dose over the 12:12 light-dark cycle that was applied in the experiment. The UV signal was not perfectly homogeneous over each tank (it dropped at the periphery), but constant water flow and constant mixing of the eggs ensured equivalent cumulative exposure over the course of the experiment.

The UV targeted daily doses (290–400 nm) was 600 kJ m^{-2}. The bulbs delivered this amount of UV radiation over 12 h at an average flux of 14 ± 2 W m^{-2}. This value is representative of surface level irradiance at the beginning of April in the Lofoten Archipelago (Fig. S3). The UV irradiance levels used in this experiment were representative of worst-case scenarios under contemporary conditions at the spawning grounds in Lofoten. The target values were determined based on data from the ALOMAR observatory at Andenes (Andøya, Lofoten, 69°18′N) and the U.S. National Science Foundation observatory at Barrow, Alaska (71°19′N), which are located at similar latitudes (http://uv.biospherical.com/login/data_overview.asp). The reference data is taken from NSF's monitoring network station at Barrow, Alaska (71°N). These data are comparable to the published meteorological data from Andøya (a scaled UV index).

The oil concentrations used were selected to mimic high oiling following a major oil spill disaster. For comparison, the PAH concentrations in close proximity to the Exxon Valdez and Deepwater Horizon oil spill were 40 and 100 μg PAH/L, respectively, while the concentration in the surroundings were 0.1–10 μg PAH/L (Boehm et al., 2016; Boehm et al., 2007). Considering that PAHs make up about 1% of the crude oil (Meador and Nahrgang, 2019), this corresponds to 1–100 μg oil/L. Crude oil was obtained from SINTEF Materials and Chemistry (Trondheim, Norway) and originates from the Troll field in the North Sea. Before exposure, the crude oil was heated for about 2 h to 200 °C in order to remove light and volatile substances present in crude oil, similar to what would evaporate from the sea surface after 2–7 days at around 10 °C air temperature (Nordtug et al., 2011). Crude oil and seawater were pumped together into the exposure tanks using a HPLC pump (Pharmacia, LKB2150) with a flow of seawater of 180 mL/min. Seawater with oil droplet concentration was 32 mg crude oil per L. The exposure concentration in the tanks was regulated by a parallel pipeline system with one line of clean seawater flow and the other line containing the crude oil. The two pipelines were connected by a three-way magnetic valve allowing water to be collected from both lines. Different dilutions were produced by controlling the relative sampling time from the oil stock solution and clean water, respectively, using a computer-controlled relay (MiniBee card and BeeStep software). The flow rate through the tanks was 32 L/h. The experimental setup consisted of a control group and five oil treatment groups: Control (NC), Control + UV (UVC), 3 μg/L (N1/UV1), 13 μg/L (N2/UV2), 50 μg/L (N3/UV3), 200 μg/L (N4/UV4), and 600 μg/L (N5/UV5) with and without co-exposure of UV radiation (denoted as N(1–5) and UV(1–5), respectively). Embryos were snap-frozen in liquid nitrogen and kept at −80 °C until the analyses were conducted.

2.3. Chemical analyses

One liter of water was collected from each exposure tank at the beginning and end of the oil exposure window. Water samples were extracted with internal standards using liquid-liquid extraction with two 1 mL volumes of dichloromethane and dried with 0.2–0.4 g Na_2SO_4. Extracts were reduced to 200 μL and solvent-exchanged into isooctane before quantitation. For body burden samples, 50–100 eggs were collected at the conclusion of the oil exposure window from each treatment and replicate, and snap frozen in liquid nitrogen until extraction. After the addition of internal standards, the samples were homogenized and extracted as described previously (Sørensen et al., 2016b). Briefly, samples were extracted twice using 3 mL of 1:1 *n*-hexane:dichloromethane and dried using 0.2–0.4 g Na_2SO_4. Samples were cleaned-up using Chromabond SiOH solid phase extraction columns (3 mL, 500 mg, Machery-Nagel, Germany), and eluted with 9:1 *n*-hexane:dichloromethane (Sørensen et al., 2016a). Final extracts were reduced to 50–100 μL before quantitation. Quantitative analyses of water and body burden samples were performed on an Agilent 7890 gas chromatograph coupled to an Agilent 7010c triple quadrupole mass detector (GC–MS/MS) as described in Sørensen et al. (2016b). The analytical method includes 61 individual PAHs and 24 clusters representing sums of alkylated PAHs (Tables S1 & S2).

Linear regressions were used for modeling the relationship between 1) sum of PAH (ΣPAH) concentration in water and ΣPAH in body burden samples, and 2) ΣPAH in body burden and *cyp1a* gene expression in embryos and larvae. Statistical differences between experiments were assessed by analyzing the interaction between the predictor variables using ANOVA analyses in R v1.2.1335 software. Benchmark doses for 10% mortality were modelled and calculated using the PROASTweb module, Version 70.1 (https://proastweb.rivm.nl).

2.4. Quantitative polymerase chain reaction analyses (qPCR)

Total RNA was isolated from ten pooled samples of embryos from each tank ($n = 3$) at 6 dpf using the TRI Reagent® protocol (Sigma-Aldrich, St. Louis. Missouri, United States) as outlined by (Chomczynski, 1993). DNase treatment was applied using the Invitrogen TURBO DNA-free™ kit (Thermofisher, Massachusetts, United States) following the provider's protocol. 500 ng of total RNA was reverse transcribed to cDNA using the iScriptTM cDNA Synthesis Kit (Bio-Rad, California. USA) following the provider's protocol. Quantitative real-time polymerase chain reaction analyses (qPCR) were performed using a CFX96 Touch Real-Time PCR Detection System (Bio-Rad, California. USA) as described in Aranguren-Abadía et al. (2020a, 2020b). The reference genes elongation factor 1 alpha (*ef1a*) and ubiquitin (*ubi*), were used for normalization of gene expression in embryos. The normalization factor was calculated based on the geometric mean using the geNorm software (Vandesompele et al., 2002). The geNorm stability index M was below one for the reference genes from both experiments. Relative expression of *ahr1a*, *ahr2a*, *cyp1a*, *ahrrb*, *cyp3a166* and *cyp24a1* genes (Table 1) was analyzed on log transformed fold-change data using a one way ANOVA and Dunnet's multiple comparison tests in R v1.2.1335 software (Crawley, 2012).

2.5. RNA-seq analyses

RNA samples from NC, N4, N5, UVC, UV4 and UV5 groups at 6 dpf were submitted for sequencing to the Genomics Core Facility at the University of Bergen, using the Illumina HiSeq 4000 platform (Illumina. Inc., San Diego, CA, USA). The final cDNA library was sequenced to generate

Table 1
Primers used for quantitative PCR (qPCR) analyses in Atlantic cod embryos.

Gene	Accession number	Forward primer (5′-3′)	Reverse primer (5′-3′)
ahr1a[a]	MN329012	CAAGGGCGTCTCAAGTTCCTACAT	CAGCACTATCTTCCCCTTTGCATCAC
ahr2a[a]	MN329013	ACAAACTGTCCGTGCTCCGACTTA	TCCATTCGGGCCATTGTGCTTCT
cyp1a[a]	ENSGMOG00000000318	CACCAGGAGATCAAGGACAAG	GCAGGAAGGAGGAGTGACGGAA
ahrrb[a]	ENSGMOG00000009114	GTGTCCCCCACAACACAAGG	GAGTGGAAGAGATTGCTCACCA
cyp3a166[b]	ENSGMOG00000007792	GCATACAAACGAGGCTTTACC	TGAGGGAGACATCTGTGGTG
cyp24a1	ENSGMOG00000010010	TCTTCAGCACAGCCAAGGT	GTCGCGTACAGCTCCTTCTT
ef1a[a]	ENSGMOG00000012005	CATCAACATCGTGGTCATT	ATGGTTCTCTTGTCAATGC
ubi[c]	EX735613	GGCCGCAAAGATGCAGAT	CTGGGGCTCGACCTCAAGAGT

[a] (Aranguren-Abadía et al., 2020a, 2020b).
[b] (Eide et al., 2018).
[c] (Olsvik et al., 2008).

50 million 75 bp paired-end reads per sample. The resulting data were analyzed as described in Yadetie et al. (2018), using the RNA-Seq analysis workflow adapted from RASflow (Yadetie et al., 2018; Zhang and Jonassen, 2020). The quality of the reads was checked using FastQCv0.11.8 (http://www.bioinformatics.babraham.ac.uk/projects/fastqc). The reads of 18 high-quality sequenced samples in total (n = 3 per group), were aligned to the Atlantic cod (gadMor1) reference genome (gadMor1 from Ensembl, (Star et al., 2011)) using HISAT2 v2.1.0 (Kim et al., 2015; Kim et al., 2019). Reads were then counted using featureCounts from Subread v1.6.4 (Liao et al., 2014). Only the genes with expression levels over one count per million (cpm) in at least one sample in the compared groups were kept. Normalization was performed by Trimmed Mean of M values afterwards (Robinson and Oshlack, 2010). Differential expression analysis was performed using edgeR v3.26.0 (McCarthy et al., 2012). Genes with False Discovery Rate (FDR) < 0.01 and a fold-change of expression (compared to controls) of at least 2.0 were considered differentially expressed genes (DEGs). Some individual genes involved in different physiological functions that were not part of the enriched pathways (see below) were identified manually from the DEGs lists.

2.6. Pathway analysis

Pathway analysis was performed as described in Yadetie et al. (2018). Briefly, human or zebrafish orthologs of Atlantic cod genes were retrieved from the Ensembl database (ensembl.org). Pathway and network enrichment tools and databases such as String (Szklarczyk et al., 2019), Metascape (Zhou et al., 2019) and Enrichr (Chen et al., 2013; Kuleshov et al., 2016) were used for functional analysis of DEGs.

2.7. Multivariate statistical analyses

Principal component analysis (PCA) and hierarchical clustering were performed in Qlucore Omics Explorer (Qlucore Omics Explorer, Qlucore AB, Lund, Sweden). RNA-Seq data (log2-transformed, normalized cpm values) from control and exposed samples (total 18, n = 3 per group) were used. Multi Group Comparison at FDR (q-value) < 0.05 was performed for PCA and hierarchical clustering.

2.8. Imaging and video analyses

Videos of 3 days post hatching (dph) larvae were taken with an Olympus SZX-10 Stereomicroscope equipped with a Moticam 1080 camera (Motic®, Richmond, BC, Canada). Larvae were immobilized in 3% methylcellulose and positioned on a thermally regulated microscope stage (Brook Industries, Illinois, United States) at 6 °C. Images and twenty second-long live videos were digitized at 30 frames/s using the Motic Live Imaging Module. Length of jaw, ethmoid plate, fin fold and ventricle diastolic (D) and systolic (S) areas were measured using Image-J (Image-J 1.52t, National Institutes of Health, Bethesda, Maryland, USA) with the Object J plugin as described in Sørhus et al. (2016). Ventricle fractional shortening (FS) was calculated as follows: (Fractional Shortening = (Diastolic area(D) − Systolic area(S))/Diastolic area(D)) (Sørhus et al., 2016). Differences in length of jaw ethmoid plate, fin fold, D and S areas, and FS between control and exposed samples were tested using one-way ANOVA and Dunnett's multiple comparison tests in R v1.2.1335 software. Additionally, presence of spinal curvature deformities and silent heart were also assessed, and differences were calculated using a chi-square test in R v1.2.1335.

3. Results

3.1. Water chemistry, body burden, gene expression, and mortality

Water chemistry, body burden and *cyp1a* expression were analyzed in Atlantic cod 6 dpf embryos after 72 h of exposure to crude oil with and without exposure to UV radiation (Fig. 1). In tanks with the same nominal crude oil concentrations, we observed differences in measured concentrations in the water between crude oil and crude oil with UV treatments. Therefore, instead of directly comparing nominal concentrations between the two light regimes, we compared concentration-dependent responses among all the crude oil concentrations used. Induction of *cyp1a* was used as a biomarker for PAH exposure, and the effect of ΣPAH water concentration on *cyp1a* expression was similar between both experiments (p = 0.18 interaction) (Fig. 1A).

Body burden concentrations generally increased in a concentration-dependent manner in embryos exposed to crude oil alone or with additional UV radiation (Fig. 1B). The highest body burden of measured ΣPAH was observed in embryos treated only with crude oil, despite the concentrations in water being lower when compared to water samples obtained from the oil with UV treatments. Notably, the body burden was affected by the light regime, where the effect of ΣPAH water concentration on ΣPAH body burden was stronger in the crude oil only treatments, in comparison to the crude oil with UV treatments (p < 0.001 interaction) (Fig. 1B). On the other hand, the effect of ΣPAH body burden on *cyp1a* expression was stronger in embryos co-exposed to crude oil with UV radiation (p < 0.001 interaction) (Fig. 1C).

The effect of ΣPAH water concentration on *cyp1a* expression was also similar between experiments for both the 2- and 3-ring PAHs (Fig. S4A) and 4+-ring PAHs (Fig. S5A). However, most of the 2- and 3-ring PAHs bioaccumulated significantly more in the crude oil alone experiment (p < 0.001 interaction) (Fig. S4B, Table S3) in comparison to 4+-ring PAHs, where ΣPAH body burden levels were similar between experiments (p = 0.12 interaction) (Fig. S5B, Table S3). No individual PAH parent

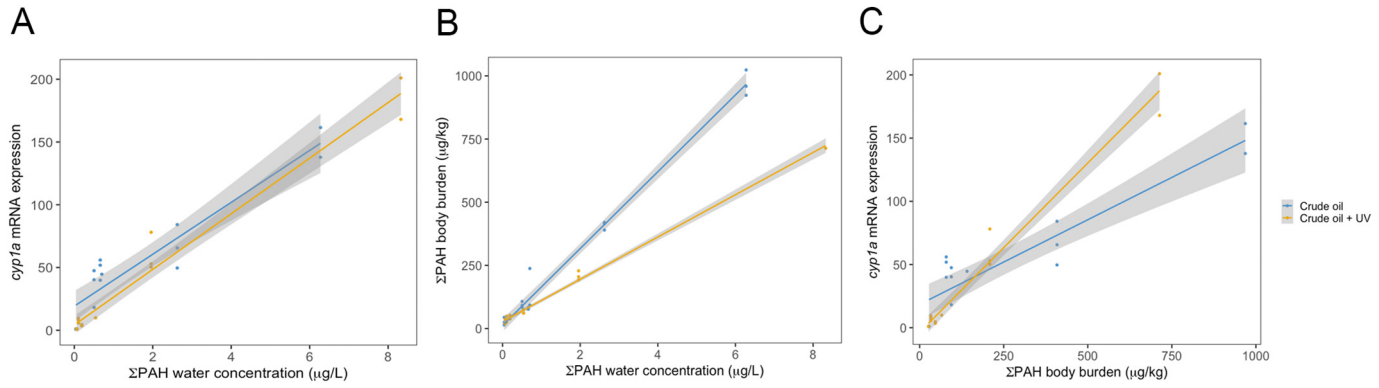

Fig. 1. Gene expression and chemical analyses in 6 days post hatching (dpf) Atlantic cod (*Gadus morhua*) embryos after 72 h of exposure to different crude oil concentrations with and without UV radiation. A) *cyp1a* mRNA expression relative to concentration of ΣPAH in water was used as a biomarker of exposure. B) Body burden of measured ΣPAH accumulation relatively to concentration ΣPAH in water and C) *cyp1a* mRNA expression relatively to body burden of measured ΣPAH levels. Linear regression models and ANOVA analyses were performed in R v1.2.1335 software. Shaded areas represent confidence intervals.

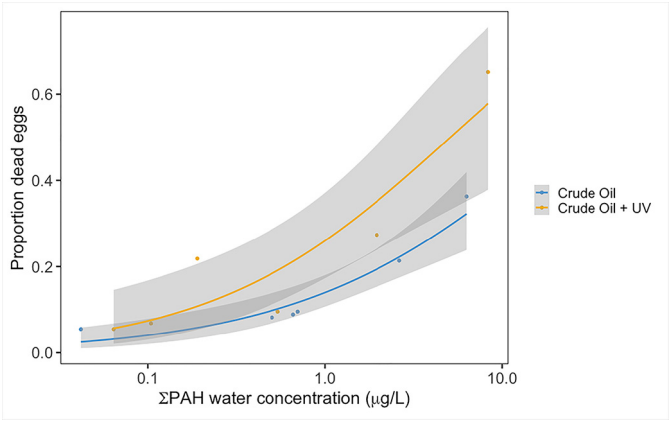

Fig. 2. Acute mortality of Atlantic cod (*Gadus morhua*) embryos after crude oil exposure with or without UV radiation. Proportion of dead eggs was measured in 6 days post fertilization (dpf) Atlantic cod embryos after 72 h of exposure. Embryos were exposed to different crude oil concentrations with and without UV radiation as indicated. Logistic regressions were performed using generalized linear models in R v1.2.1335 software. Differences between experiments were assessed with ANOVA analyses. Shaded areas represent confidence intervals.

compound, or the different alkylated PAH clusters, bioaccumulated more in the presence of UV (Table S3). However, differences in *cyp1a* expression between experiments were observed in both individual 2- and 3-ring PAHs ($p < 0.001$ interaction) (Fig. S4C) and 4+-ring PAHs ($p < 0.001$ interaction) (Fig. S5C), where the effect of ΣPAH body burden on *cyp1a* expression was stronger in the crude oil with UV treatments.

Acute mortality was detected in both experiments with increasing concentrations of measured ΣPAH in water (Fig. 2). Higher mortality was observed in embryos co-exposed to crude oil and UV radiation at the higher crude oil concentrations used. The benchmark dose (BMD_{10}) for the crude oil experiment was between 4.4 and 4.6 μg/L ∑PAH (derived from 3 models). The BMD_{10} for the co-exposure experiment was between 4.02 and 4.15 μg/L ∑PAH (derived from 2 models). The light regime did not enhance the overall toxic effect of ΣPAH present in water ($p = 0.76$ interaction), since the proportion of dead eggs was similar between experiments at the lower doses (Fig. 2).

3.2. Analyses of phenotypic traits

Morphological effects were clearly visible in 3 dph cod larvae exposed to crude oil with and without UV radiation at the highest doses (N5 and UV5) (Fig. 3). Notably, craniofacial malformations were predominant, and the ethmoid plate and jaw length were significantly

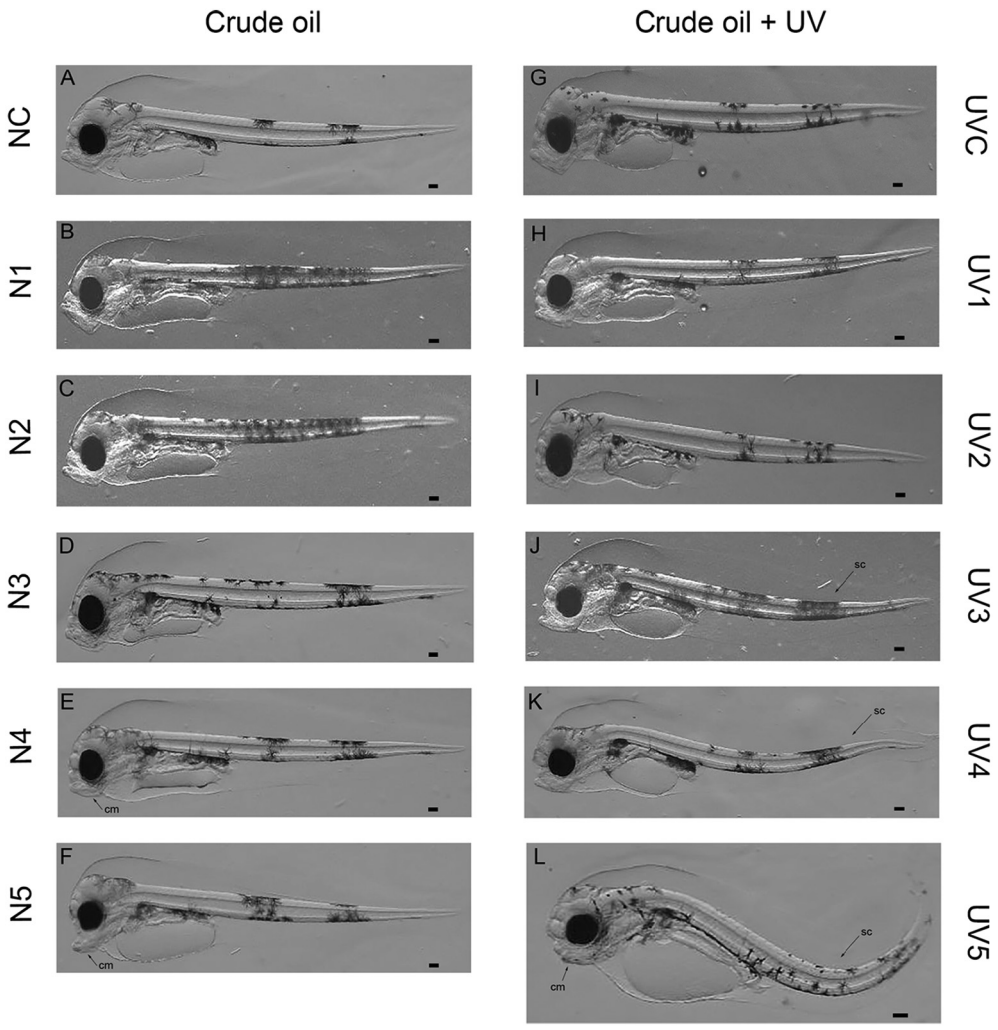

Fig. 3. Phenotypic analyses of Atlantic cod (*Gadus morhua*) larvae. A) NC and B–F) crude oil exposed larvae 3 days post hatching (dph), G) UVC and I–L) crude oil with UV radiation exposed larvae 3 dph. Scale bars represent 100 μm. cm: craniofacial malformation, sc: spinal curvature. Control (NC), Control + UV (UVC), 3 μg/L (N1/UV1), 13 μg/L (N2/UV2), 50 μg/L (N3/UV3), 200 μg/L (N4/UV4), and 600 μg/L (N5/UV5). Crude oil concentrations are nominal.

Table 2
Phenotype analyses in Atlantic cod (*Gadus morhua*) 3 days post hatching (dph) larvae. Differences in ethmoid plate, jaw and fin fold length, and spinal curvature between exposed larvae and its respective control were measured using one-way ANOVA and Dunnett's multiple comparisons tests in R v1.2.1335 software. Presence of spinal curvature was calculated using a chi-square test. Statistical differences are indicated with *($p \leq 0.05$), **($p \leq 0.01$) or ***($p \leq 0.001$).

Treatment	Nominal crude oil concentrations	Ethmoid plate (μm)	Jaw length (μm)	Fin fold (mm)	Spinal curvature (%)
NC	0 μg/L	123 ± 18	374 ± 29	3.5 ± 0.9	0
N1	3 μg/L	121 ± 19	365 ± 22	3.4 ± 1.1	0
N2	13 μg/L	128 ± 19	358 ± 28	3.2 ± 0.8	0
N3	50 μg/L	116 ± 14	337 ± 52*	2.6 ± 0.8**	0
N4	200 μg/L	111 ± 14*	302 ± 36***	3.1 ± 1.0	0
N5	600 μg/L	93 ± 26***	295 ± 50***	2.8 ± 0.9*	6
UVC	0 μg/L + UV	118 ± 18	366 ± 32	3.5 ± 2.6	17
UV1	3 μg/L	120 ± 17	347 ± 30	3.7 ± 0.8	17
UV2	13 μg/L	119 ± 15	347 ± 39	3.9 ± 1.1	10
UV3	50 μg/L	123 ± 18	337 ± 27*	3.4 ± 1.2	33**
UV4	200 μg/L	112 ± 16	358 ± 27	2.5 ± 0.6*	35**
UV5	600 μg/L	110 ± 17	304 ± 36***	1.8 ± 0.6***	69***

shortened (N5 and UV5) (Table 2). Malformations were also observed in the head and mouth from N4 larvae, and there was also a significant shortening of the ethmoid plate and jaw length (Tables 2 & 4). Deformities in spinal curvature were in general present in the larvae co-exposed to UV radiation (UV1–5), including larvae from the control group (UVC) (Tables 2 & 4). However, significantly increased and more severe deformities were observed in larvae exposed to the three highest crude oil concentrations with UV, i.e. groups UV5 (69%), UV4 (35%) and UV3 (33%) (Fig. 3J, K, L) (Table 2), where a scoliosis phenotype was predominant in UV5 larvae (Fig. 3L). The fin fold area was significantly reduced in larvae from N5, N3, UV5 and UV4 groups, indicating pronounced effects on the fin formation (Tables 2 & 4). Some deformities were also observed at the lowest crude oil concentrations, where significantly shortened jaw length was evident in larvae from both the N3 and UV3 groups (Table 2).

Larvae from both experiments showed heart deformities at the highest crude oil concentrations (N5 and UV5), including significantly decreased diastolic (D) and systolic (S) area of the ventricle, as well as ventricular fractional shortening (FS) (Tables 3 & 4). The proportion of individuals with a silent ventricle was also significantly higher in larvae from these groups (N5 = 47% and UV5 = 30%) (Tables 3 & 4). Larvae from the N4 group also had a significantly smaller S area and higher FS, whereas there was only a decrease in the diastolic area in UV4 larvae (Tables 3 & 4). There were also significant changes at the low crude oil concentrations, where FS was higher in larvae from N2 and UV1 groups compared to the control groups (Table 3).

Table 3
Cardiac analyses in Atlantic cod (*Gadus morhua*) 3 days post hatching (dph) larvae. Differences in ventricle diastolic area, ventricle systolic area and ventricular fractional shortening between exposed larvae and its respective control were measured and statistically compared using one-way ANOVA and Dunnett's multiple comparisons tests. Differences in silent ventricle were assessed using a chi-square test tests in R v1.2.1335 software. Statistical differences are indicated with *(p ≤ 0.05), **(p ≤ 0.01) or ***(p ≤ 0.001).

Treatment	Nominal crude oil concentrations	Ventricle diastolic area (mm^2)	Ventricle systolic area (mm^2)	Silent ventricle (%)	Ventricular fractional shortening (%)
NC	0 μg/L	7.0 ± 1.2	5.6 ± 0.8	7	18.8
N1	3 μg/L	6.7 ± 1.1	5.1 ± 0.9*	7	28.4
N2	13 μg/L	7.0 ± 1.1	5.2 ± 0.8	0	24.2*
N3	50 μg/L	7.0 ± 11.7	5.3 ± 0.9	0	23.1
N4	200 μg/L	6.5 ± 1.0	4.7 ± 0.6***	3	26.1**
N5	600 μg/L	4.9 ± 1.3***	4.3 ± 0.8***	47***	10***
UVC	0 μg/L + UV	6.8 ± 1.3	5.5 ± 1.1	10	18.9
UV1	3 μg/L	6.5 ± 1.3	4.8 ± 1**	10	25.8*
UV2	13 μg/L	7.2 ± 1.0	5.6 ± 0.7	3*	22
UV3	50 μg/L	6.3 ± 0.9	5.0 ± 0.7	10	21.3
UV4	200 μg/L	6.0 ± 0.9**	5.0 ± 0.7	7	16.7
UV5	600 μg/L	4.7 ± 0.8***	4.1 ± 0.6***	30***	11.2**

3.3. Transcriptomic responses in exposed Atlantic cod embryos

3.3.1. Differentially expressed genes (DEGs)

RNA-seq analyses were performed to reveal alterations in gene expression in cod embryos exposed to crude oil alone, or crude oil combined with UV radiation using a factorial design in edgeR (McCarthy et al., 2012). The number of DEGs with a fold-change of at least 2 (expression ratio ≥ 2 for up-regulated, expression ratio ≤ 0.5 for down regulated, and an FDR < 0.01) was 413 and 116 in the N5 and N4 crude oil exposed groups, respectively (Fig. 4A, Tables S4–S5). In comparison, 1452 and 279 DEGs were identified in the UV5 and UV4 crude oil exposed groups with UV radiation, respectively (Fig. 4B, Tables S6–S7). The co-exposure of oil with additional UV radiation resulted in a higher number of DEGs compared to crude oil exposure alone. Both the N4 and UV4 exposed groups shared the majority (over 85%) of the DEGs with their corresponding groups exposed to the highest crude oil concentration (N5 and UV5), demonstrating a strong dose-response trend in the datasets (Fig. 4A & B). About one-third of the DEGs in the groups treated solely with crude oil are shared with the groups co-exposed to UV radiation (Fig. 4C & D). Only 70 DEGs were identified in the UV-only (UVC versus NC) treatment group, most of which were shared with the UV5 group (Fig. S6, Table S9).

Table 4
Summary of the different phenotypic outcomes and enriched pathways results. Table A) shows observed phenotypes in embryos exposed to crude oil with and without UV radiation. Table B) shows enriched pathways in the transcriptome of embryos exposed to crude oil with and without UV radiation, and those found in the interaction analysis. "X" indicates presence of a result. Crude oil: N4 (200 μg/L), N5 (600 μg/L); Crude oil + UV:UV4 (200 μg/L + UV), UV5 (600 μg/L + UV) groups.

A)

Phenotype	N4	N5	UV4	UV5
Ethmoid plate	x	x		
Jaw	x	x		x
Ventricle size	x	x	x	x
Ventricle contraction	x	x		x
Silent ventricle		x		x
Fin fold		x	x	x
Spinal curvature			x	x
Increased mortality			x	x

B)

Pathway	N4	N5	UV4	UV5	Interaction
Muscle contraction	x	x			
Ahr signaling pathway	x	x	x	x	
Circadian rhythm			x	x	x
Oxidative stress			x	x	x
Tryptophan metabolism			x	x	x
Vitamin A and D pathways			x	x	x

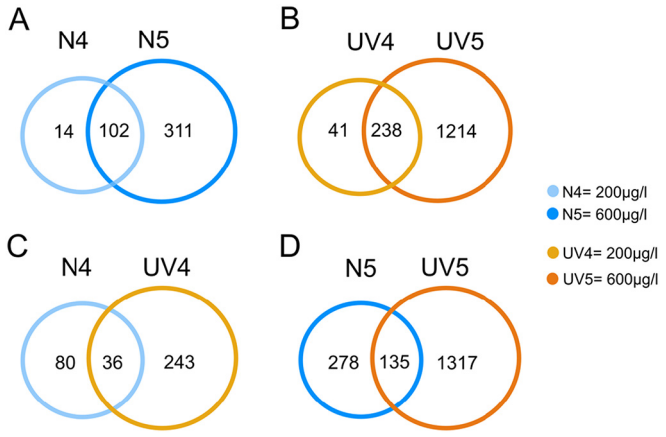

Fig. 4. Venn diagrams comparing differentially expressed genes (DEGs) in Atlantic cod (*Gadus morhua*) embryos in the different treatment groups (A–D). At least 2 fold-changes and FDR < 0.01 were used as a cutoff for DEGs from Atlantic cod 6 days post fertilization (dpf) embryos exposed to the different treatments as indicated. Crude oil: N4 (200 μg/L), N5 (600 μg/L); Crude oil + UV: UV4 (200 μg/L + UV), UV5 (600 μg/L + UV). Crude oil concentrations are nominal.

3.3.2. Principal component analysis (PCA) and hierarchical clustering

Principal component analysis (PCA) and hierarchical clustering analyses were performed with log2-transfomed counts per million (cpm) values of all genes as input. Filtering was performed based on ANOVA (FDR q-value < 0.05) that resulted in 318 genes discriminating the groups as shown in the PCA and the heatmap obtained from hierarchical cluster analysis (Figs. 5, S7). The heatmap shows distinct expression profiles dominated by upregulation of several genes in the co-treatment groups (UV4 and UV5) (Figs. S7–8). Many of the upregulated genes are light responsive genes involved in circadian rhythm, DNA repair, and mitochondrial iron metabolism (Fig. S9). Fig. 5 shows hierarchical clustering and PCA analyses based on a subset of genes (the top 50 most significant). The different exposure groups are well separated in the PCA according to their exposure regime, including the two separate control groups (Fig. 5A). The Ahr target genes *cyp1a*, *cyp1c2* and *ahrrb* were up-regulated in all exposed groups independent of the light regime (Fig. 5B, Tables S4–S7). Most of the top 50 genes were up-regulated only in embryos from the UV5 and UV4 groups, such as *per2* and *cry1a* (circadian regulation), *ddb2* (DNA repair and response to UV), and *ghdc* (glucose metabolism) (Fig. 5B, Tables S6–S7).

3.3.3. Analysis of interaction effect

There was a lower number of DEGs in the N4 and UV4 groups in comparison to N5 and UV5, which received the highest concentration

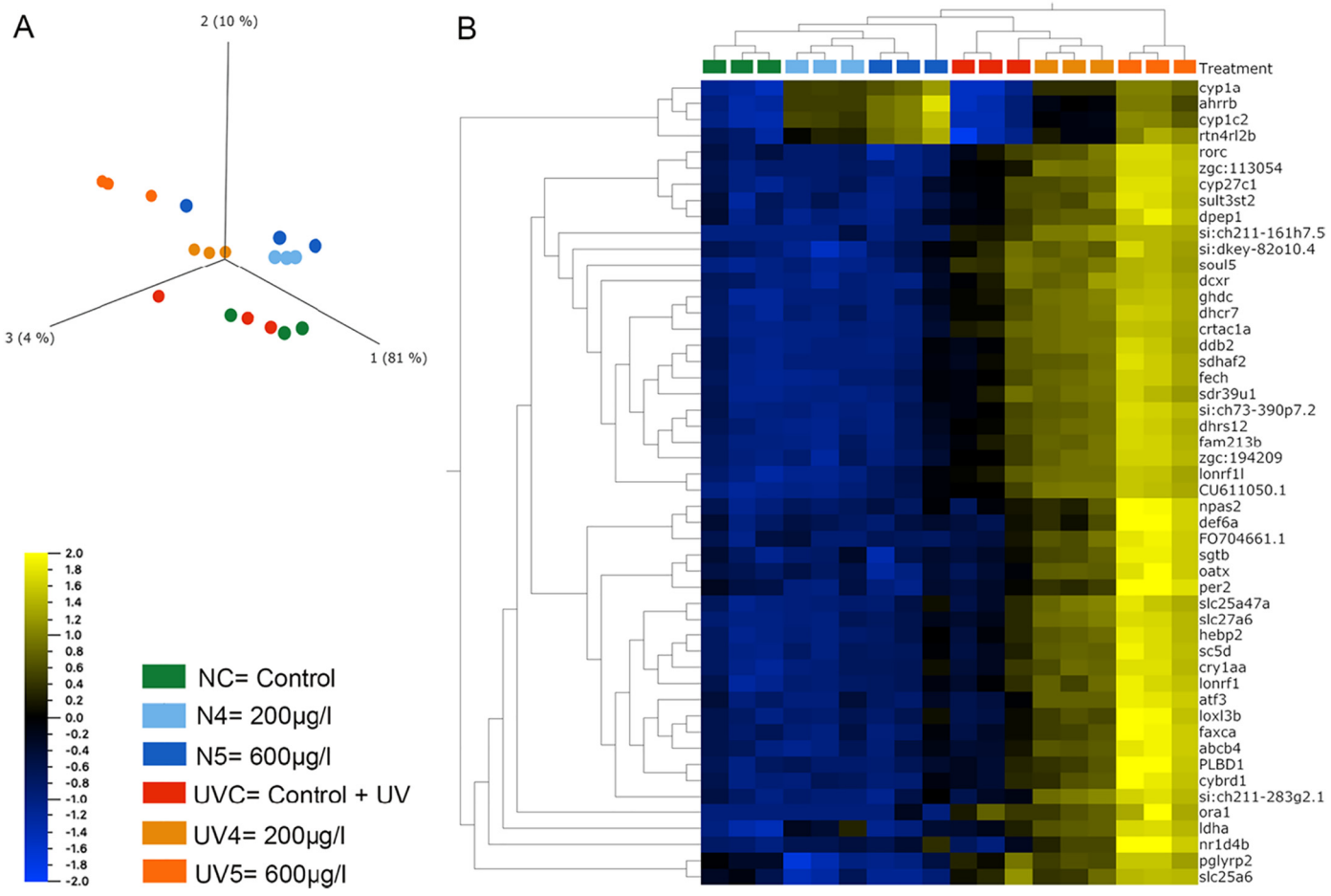

Fig. 5. Principal component analysis (A) and two-way hierarchical clustering (B) of RNA-seq data from Atlantic cod (*Gadus morhua*) embryos. Log2-transformed normalized counts per million (cpm) of RNA-seq data from Atlantic cod 6 days post fertilization (dpf) embryos exposed to the different treatments (as indicated) was used in Multi Group Comparison (ANOVA) at FDR q-value < 0.05 (Qlucore Omics Explorer). Only the top 50 genes discriminating the groups are shown in the PCA (A) and in the hierarchical clustering heatmap (B). The full list of the 318 genes in the hierarchical cluster analysis is shown in Supplementary Figs. S7 & S8. Relative gene expression levels are shown by the color scale bar (bottom left), with blue and yellow ends indicating lowest and highest expression levels, respectively. Crude oil: NC (control), N4 (200 μg/L), N5 (600 μg/L); Crude oil + UV:UV (Control + UV), UV4 (200 μg/L + UV), UV5 (600 μg/L + UV). Crude oil concentrations are nominal.

of crude oil (Fig. 4A & B). Therefore, we conducted the oil and UV interaction effect analysis only on the N5 and UV5 groups. We conducted a statistical test to investigate the interaction between the crude oil and UV radiation treatments using a full factorial design (highest crude oil concentration * UV radiation) and factorial ANOVA analyses. We used edgeR v3.26.0 (McCarthy et al., 2012) to test the interaction between high crude oil concentration and UV radiation with the design formula: ~oil * UV (equal to ~oil + UV + oil:UV, where oil has two levels: "control" and "high", and uv also has two levels: "no" and "yes"). The genes with FDR < 0.0001 were considered significant, and a total of 907 DEGs were affected by the interaction effect with this cutoff (Table S8). Most of the genes identified as up-regulated in the co-exposure groups (UV4 and UV5) are also a subset of the genes identified in the interaction effect analysis (Figs. 5B and S8–9).

3.3.4. Pathway analyses

Pathway enrichment analyses were performed separately on DEGs identified from either the crude oil groups (N5 + N4) (Tables S4–S5), the combined crude oil and UV treatment groups (UV5 + UV4) (Tables S6–S7), and on DEGs affected by the interaction effect of crude oil and UV radiation (Table S8). The pathway analysis results summarized in this section are presented in Tables S10–S12 and Fig. S10. Ahr signaling pathway genes such as *cyp1a* are the top induced genes shared between crude oil and combination treatments (Fig. 5B). The top pathways affected in the crude-oil treatment group appear to be largely related to Ahr signaling, muscular contraction and vasoconstriction (Fig. S10, Table S10). The Ahr signaling pathway is also shared with the co-exposed groups (Fig. S10, Tables 4–5, Table S11). Longer lists of pathways were significantly affected in UV5 treatment group and by the interaction effect, compared to the N5 treatment group. The majority of the pathways are common between the UV5 group and interaction effect analysis (Fig. S10, Tables 4 & 5, Tables S11–S12). The crude oil treatment shared fewer pathways with the UV5 group and interaction effect analysis (Fig. S10, Tables 4 & 5, Tables S10–S12). In the UVC group, enrichment of some metabolic and light response related pathways, as well as tryptophan metabolism pathway were observed and were shared mostly with the combination treatment (Figs. S10 & S11, Table S13). Many of the pathways affected in the co-exposed groups and detected in the interaction effect analysis are dominated by pathways related to circadian rhythm and oxidative stress responses

Table 5
Selected gene responses in 6 days post fertilization (dpf) Atlantic cod embryos after exposure to crude oil with or without UV radiation. Upregulated (yellow) and downregulated (blue) genes and associated pathways from crude oil exposed N5 (600 μg/L) and UV5 (600 μg/L + UV) groups and interaction analyses DEGs lists. The physiological role the enriched pathway is associated to is indicated in parentheses.

Function/(Pathway)	ZF ID	Crude oil	Crude oil + UV	Interaction	Zfin annotation
Heart muscle contraction (muscular contraction)	*cacna1a*[a,b,c]				L-type Ca^{2+} channels (Ltcc) alpha 1sa
	ryr3[a,b,c]				Ryanodine receptor 3
	tnnc2				Troponin C type 2
	myh7bb				Myosin heavy chain 7b
Heart cells proliferation (muscular contraction)	*myl7*[d,e,f]				Myosin light chain 7
Heart cells differentiation (muscular contraction)	*myh6*[d,e,f]				Myosin heavy chain 6
	bmp2b[g]				Bone morphogenetic protein 2b
Craniofacial development	*foxq1a*[h]				Forkhead box Q1a
	dlx4[i]				Distal-less homeobox 4a
	pax9[j]				Paired box 9a
Nrf2 pathway (oxidative stress)	*nfe2l2a*				Nuclear factor erythroid 2a
	keap1b				Kelch-like ECH-associated protein 1b
	prdx1				Peroxiredoxin 1
	gsr				Glutathione reductase
	gclc				Glutamate-cysteine ligase, catalytic subunit
	gclm				Glutamate-cysteine ligase, modifier subunit
	gsta.1				Glutathione S-transferase, alpha tandem duplicate 1
	gstt1a				Glutathione S-transferase theta 1a
	gstr				Glutathione S-transferase rho
	gstz1				Glutathione S-transferase zeta 1
Mitochondrial calcium transport (oxidative stress)	*vdac2*[l,m]				Voltage-dependent anion channel 2
	vdac3[l,m]				Voltage-dependent anion channel 3
	hspa9[l,m]				Heat shock protein 9
Ahr pathway[n]	*ahr2a*				Aryl hydrocarbon receptor 2a
	cyp1a				Cytochrome P450, family 1, subfamily A
	ahrrb				Aryl hydrocarbon receptor repressor b
Vitamin D pathway[o]	*cyp24a1*				Cytochrome P450, family 24, subfamily A
	cyp2r1				Cytochrome P450, family 2, subfamily R

[a](Brette et al., 2014), [b](Brette et al., 2017), [c](Incardona, 2017), [d](Berdougo et al., 2003), [e](Glickman and Yelon, 2002), [f](Yelon et al., 1999), [g](Reiter et al., 2001), [h](Planchart and Mattingly, 2010), [i](Coffin Talbot et al., 2010), [j](Swartz et al., 2011), [k](Kensler et al., 2007), [l](Görlach et al., 2015), [m](Honrath et al., 2017), [n](Aranguren-Abadía et al., 2020a), [o](Lock et al., 2010).

(Tables 4–5, Fig. S10, Tables S11–S12). The retinol/vitamin A pathway was also enriched in the co-exposed groups and in interaction analysis. Thus, the general pattern appears to be Ahr signaling and development related pathways that were shared between crude oil and co-exposed groups, while several oxidative stress related pathways dominate in the combined treatment groups, largely attributed to interaction effects (Fig. S10). The list of oxidative stress related GO biological processes that were affected in a coordinated manner in the combination treatment include reactive oxygen species metabolic process, protein folding, iron-sulfur cluster assembly, heme biosynthetic process and sulfur amino acid metabolic process (Fig. S10, Table S11). These processes are populated by overlapping list of genes encoding proteins involved in oxidative stress responses such as enzymes in the Nrf2 signaling pathway (e.g. GCLM, GSTA3, GSTT2, HSP90AA1), chaperones, heatshock proteins, and anti-oxidant enzymes (Tables 4–5, Table S11). Other processes affected in the combination treatment are related to mitochondria structure and function and energy metabolism (Tables 4 & 5, Fig. S10, Table S11).

3.3.5. Quantitative polymerase chain reaction (qPCR) analyses

Differential expression of *ahr1a*, *ahr2a*, *cyp1a*, *ahrrb*, *cyp3a166* and *cyp24a1* in embryos from all groups from both experiments was also assessed with quantitative polymerase chain reaction (qPCR) analyses (Fig. 6). qPCR results confirmed RNA-seq data, with only a few exceptions. Induction of *ahr2a* and *cyp3a166* expression was found in UV4 and UV5, respectively, but this was not revealed in the RNA-seq data. Notably, qPCR data showed gene induction in the lower crude oil concentrations from both experiments, which was not assessed with RNA-seq. Significant up-regulation of *ahr1a* was only observed in the experiment with crude oil alone (Fig. 6A, B) with the lowest concentration used (N1) (Fig. 6A), while *ahr2a* induction was observed at the lowest concentrations from both experiments (N1, N2, UV1 and UV2) (Fig. 6C, D). In general, concentration-response trends in the expression levels of the Ahr target genes *cyp1a* and *ahrrb* were observed in embryos exposed to crude oil alone and the UV co-exposure experiments (Fig. 6E, F, G, H). Expression of *cyp3a166* was more predominant in the crude oil only exposure (N1 and N2) in comparison to co-exposure with UV radiation (UV2) (Fig. 6I, J). Significant induction of *cyp24a1* was detected in the co-exposure experiment (UV5) (Fig. 6K, L).

4. Discussion

Chemical analyses, acute mortality, gene expression, and phenotypic traits were different between the exposure regimes. Embryos exposed to crude oil with UV radiation had lower ΣPAH body burden levels, but *cyp1a* expression response relative to ΣPAH body burden was stronger in embryos from this experiment, which may be an indication of photomodification of absorbed PAHs. At the higher doses, mortality was higher in embryos co-exposed to crude oil and UV radiation. Some adverse outcomes, such as heart and craniofacial malformations, were observed in exposed larvae independent of the light regime. However other endpoints, such as spinal curvature deformities, were predominant and more severe in larvae co-exposed to crude oil and UV radiation, especially at the highest concentrations used. These phenotypic changes correlated well with the results from transcriptome analysis, as described in detail below.

Transcriptome analysis revealed differential effects in the crude oil and co-exposed groups with UV radiation. Genes and pathways related to many of the observed developmental malformations were affected in both crude oil and co-exposure treatments groups, consistent with the observed phenotypic outcomes in the two groups. Compared to the only crude oil treatment, the combined treatment also modulated a much larger number of genes and pathways, of which a significant portion are related to oxidative stress. The higher number of affected pathways related to toxic stress responses in the co-exposure groups may explain the increased severity of phenotypic alterations and increased mortality. Interaction effect analyses of crude oil and UV radiation confirmed that the majority of the pathways affected in the co-exposed groups were due to the photo-enhanced effect of crude oil toxicity.

4.1. Chemical analyses and cyp1a as a biomarker for crude oil exposure

Embryos from crude oil and crude oil with UV radiation exposure experiments were dosed similarly with crude oil. This is demonstrated using *cyp1a* as a biomarker of exposure, where the degree of *cyp1a* expression relative to measured ΣPAH in water was similar between experiments. Cyp1a is important for the biotransformation of PAHs in fish, and induction of *cyp1a* expression is commonly used as a sensitive biomarker of crude oil exposure (Goksøyr and Förlin, 1992b; Holth et al., 2014; Sørensen et al., 2017; Stegeman and Lech, 1991).

Photodegradation of PAHs in water induced by UV radiation is well known (Bertilsson and Widenfalk, 2002). However, the pronounced *cyp1a* gene expression responses in cod embryos suggests that co-exposure with UV radiation did not appreciably photodegrade the PAHs dissolved in the water in the 50 L flow-through tanks, which was replaced at a rate of 32 L/min with a residence time of 1.5 h. Furthermore, chemical analyses demonstrated that there were not consistent differences in dosing between delivered and nominal ΣPAH concentrations between experiments. We attribute small deviations in delivered crude oil concentrations to the oil droplet dosing system and pump.

The effect of ΣPAH water concentration on ΣPAH body burden levels suggests that accumulation of PAHs was lower in embryos exposed to crude oil with UV radiation. Analogously, accumulated PAHs (body burden) caused a stronger *cyp1a* response in the presence of UV radiation. These observations may indicate that absorbed PAHs were photomodified into new oxygen-containing and more polar molecules after they had been absorbed into the embryos (Maki et al., 2001; Ray et al., 2014; Schemeth et al., 2019; Yu, 2002). Although not included in this work, measurements of body burden of photoproducts (ketones, carboxcylic acids, and hydroxylated PAHs) would most likely be higher in embryos from the crude oil with UV radiation experiment. PAHs dissolved in water were only exposed to UV radiation quickly before the water was replaced in the flow-through system. In contrast, PAHs inside the embryos are sequestered longer under UV radiation and are more likely to be photomodified. Furthermore, when looking into the different groups of PAHs separately, 2- and 3-ring PAHs accumulated to a larger extent in embryos from the crude oil alone experiment. The PAHs present in crude oils are usually predominantly 2- and 3-ring (Bence et al., 1996; Carls et al., 1999). Even though these PAHs are poor *cyp1a* inducers (Incardona, 2017), they are more readily photomodified (Ankley et al., 1997; Arfsten et al., 1996; Wernersson, 2003). Notably, we have recently shown that hydroxylated phenanthrene and chrysenes, including 1,2-dihydrophenanthrene-1,2-diol and chrysene-1-ol, chrysene-2-ol, chrysene-3-ol, and chrysene-4-ol, act as potent cod Ahr agonists in vitro, while their unsubstituted parent compounds are not able to activate the cod Ahrs (Lille-Langøy et al. submitted). We hypothesize that PAHs may be photomodified in two ways; either PAHs induce *cyp1a* and are then photomodified, or possibly, PAHs are photomodified into compounds that induce *cyp1a* to a similar degree, such as oxygen-substituted PAHs (Wincent et al., 2015; Wincent et al., 2016).

4.2. Cardiac and craniofacial alterations

Exposure of cod embryos took place during heart morphogenesis. Myocardial and endocardial cells differentiate and begin to fuse and form the cardiac cone at 6 dpf (Hall et al., 2004). Cod larvae exposed to high crude oil concentrations (N4 and N5 groups) demonstrated reduced ventricle size and heart contraction, along with an increased number of individuals with silent ventricles. Cardiac dysfunction was also observed in larvae co-exposed to the highest crude oil

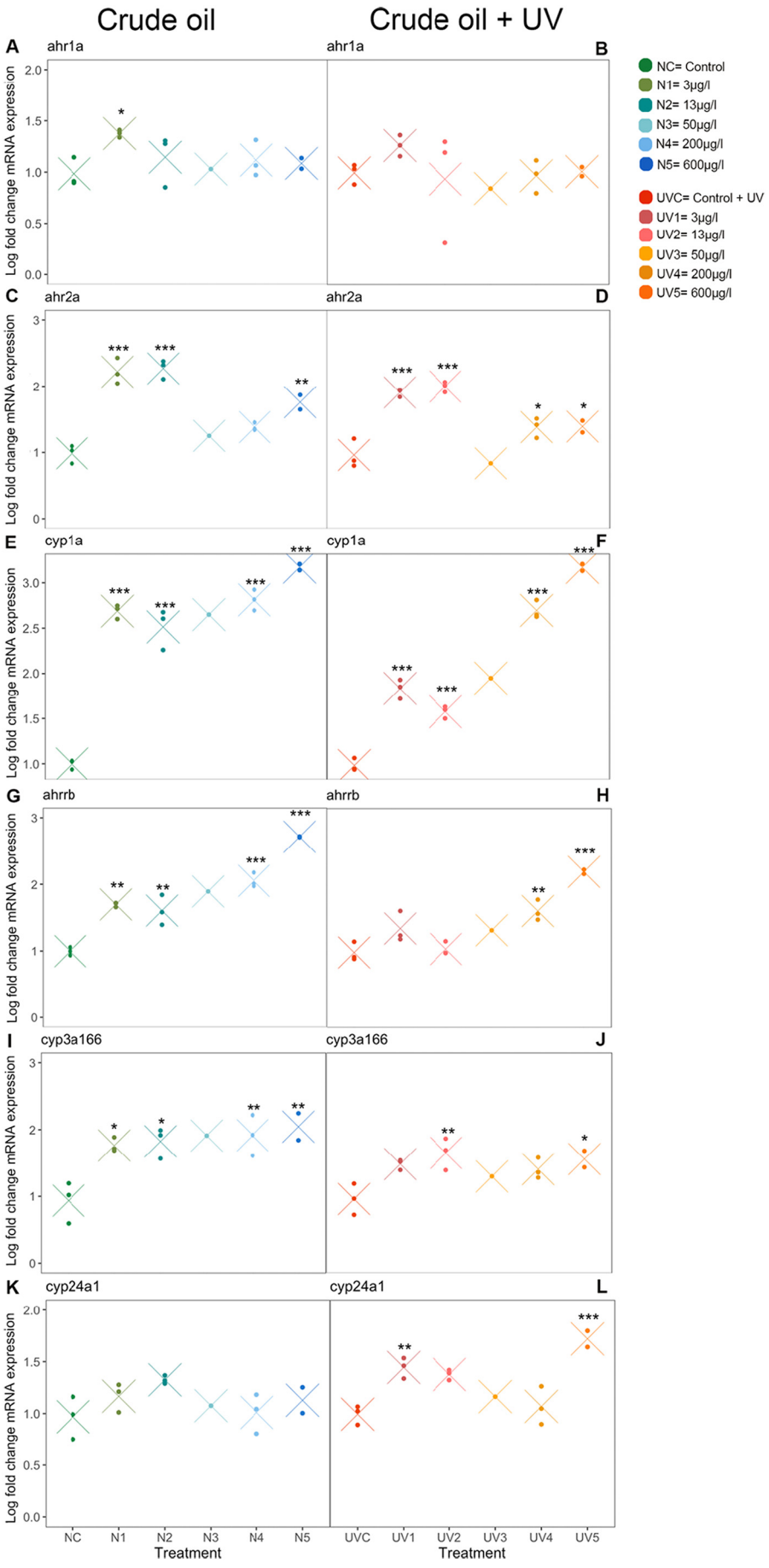
Crude oil
Crude oil + UV
A
ahr1a
B
ahr1a
C
ahr2a
D
ahr2a
E
cyp1a
F
cyp1a
G
ahrrb
H
ahrrb
I
cyp3a166
J
cyp3a166
K
cyp24a1
L
cyp24a1
Log fold change mRNA expression
NC= Control
N1= 3µg/l
N2= 13µg/l
N3= 50µg/l
N4= 200µg/l
N5= 600µg/l
UVC= Control + UV
UV1= 3µg/l
UV2= 13µg/l
UV3= 50µg/l
UV4= 200µg/l
UV5= 600µg/l
NC N1 N2 N3 N4 N5
UVC UV1 UV2 UV3 UV4 UV5
Treatment
Treatment

concentration with UV radiation (UV5 group), in addition to a decrease in ventricle size and heart contraction. Developmental cardiotoxicity is a common effect of crude oil exposure, and similar cardiac phenotypes have been observed in the ELS of several other fish species (Carls et al., 1999; Colavecchia et al., 2006; Colavecchia et al., 2004; Incardona, 2017; Marty et al., 1997; Perrichon et al., 2018; Pollino and Holdway, 2002; Sørhus et al., 2016). Shortened ethmoid plate and jaw length were also visible phenotypic outcomes induced by crude oil in larvae from the N4 and N5 groups. Similar phenotypic outcomes were also present in UV5 cod larvae, where reduced jaw length and fin fold area was observed. Craniofacial abnormalities are often associated with cardiac dysfunction, and are a secondary response to the cardiac failure produced by crude oil and TCDD (Incardona et al., 2004; Lanham et al., 2014).

4.3. Muscle contraction pathway

RNA-seq data combined with gene enrichment analyses revealed enriched pathways in muscle contraction and vasoconstriction in embryos exposed to crude oil alone (N4 and N5 groups). This is in accordance with other studies reporting altered cardiac muscular contraction in developing fish exposed to crude oil, produced largely by tricyclic PAHs in an Ahr-independent manner (Brette et al., 2014, 2017; Incardona, 2017; Sørhus et al., 2016). Abnormal myocardial cell contractions in developing fish are produced by alterations in intracellular calcium homeostasis affecting calcium transport between the sarcoplasmic/endoplasmic reticulum (SR/ER) and the muscular filaments (ibid.). Genes with important roles in calcium homeostasis and muscular formation in cardiomyocytes were also upregulated in embryos from the N5 group (Table 5, Table S5). On the other hand, downregulation of some genes involved in myocyte differentiation and proliferation, and in jaw formation were only found in co-exposed embryos from the UV5 group (Table 5, Table S7). Upregulation of the forkhead box Q1a (*foxq1a*) gene, previously found upregulated in the ELS of Atlantic haddock after crude oil exposure (Sørhus et al., 2017), was also observed in embryos from N4, N5, UV4 and UV5 groups (Table 5, Tables S4–S7). Planchart and Mattingly, 2010 reported upregulation of the paralogous gene *foxq1b* in the branchial arches of zebrafish after TCDD exposure and associated its expression with the observed craniofacial abnormalities. The Ahr signaling pathway was also enriched in N4, N5, UV4 and UV5 embryos, and Ahr-dependent cardiotoxicity is produced by some PAHs present in crude oil exposure (Cunha et al., 2020; Incardona, 2017). *cyp1a* and *ahrrb*, were upregulated in the N4, N5, UV4 and UV5 groups, while *ahr2a* expression was induced in N5, UV4 and UV5 groups. In addition, *cyp3a166* was highly upregulated in embryos from N4 and N5, and slightly in UV5 embryos. Expression of the orthologous gene *cyp3a65* is modulated by Ahr2 in zebrafish (Chang et al., 2013; Kubota et al., 2015; Tseng et al., 2005), and zebrafish *cyp3* genes appear to be regulated by both pregnane X receptor (Pxr) and Ahr2 (Kubota et al., 2015). Furthermore, in Atlantic cod, which lacks a Pxr-encoding gene, Ahr is suggested to have evolved a compensatory role in regulating *cyp3a166* expression (Eide et al., 2018). PAHs present in crude oil modulate the Ahr signaling pathway in developing cardiomyocytes of fish, producing defects in cardiac morphogenesis (Clark et al., 2010; Incardona et al., 2006; Incardona et al., 2011; Scott et al., 2011; Van Tiem and Di Giulio, 2011). Our results indicate a cardiotoxic effect of crude oil alone on cardiomyocyte muscle contraction that affects heart morphogenesis in developing cod. However, this effect is different when compared to the combined crude oil with UV radiation exposure, where UV may have affected myocardial cells differentiation and proliferation, as suggested by downregulation of genes involved in these processes. The craniofacial malformations observed in exposed cod larvae may be a secondary response to the heart abnormalities detected in cod larvae from both experiments (Incardona et al., 2004; Lanham et al., 2014).

4.4. Photo-enhanced effect of crude oil on cod embryos

Photo-enhanced toxicity of crude oil (resulting from interaction of crude-oil and UV) was clearly visible in co-exposed embryos at the high concentrations (UV4 and UV5), indicated by higher mortality and increased abundance of spinal curvature deformities, where scoliosis was the main deformity observed. Spinal deformities were also observed in co-exposed embryos from UV3 group, but there was no visible sign of photo-enhanced crude oil toxicity at the lower concentrations. The lethal BMD_{10} is estimated to correspond to approximately ~4 μg/L $\sum$PAH, which is similar to earlier observation of oil toxicity in cod (Sørensen et al., 2017). Photo-enhanced toxicity has been reported in the ELS of a number of different fish species, as well as juvenile fish exposed to crude oil and PAHs with UV radiation (Alloy et al., 2016; Barron et al., 2003; Barron et al., 2005; Barron et al., 2018; Diamond et al., 2006; Farwell et al., 2006; Hatlen et al., 2010; Incardona et al., 2012; Little et al., 2000). In marine ecosystems, exposure to UVB is considered a major environmental stressor to pelagic marine fish eggs and larvae. Studies assessing the effect of UVB exposure have reported increased mortality in a variety of fish species (Zagarese and Williamson, 2001), including Atlantic cod (Béland et al., 1999; Kouwenberg et al., 1999; Lesser et al., 2001), where exposure to solar UVB radiation causes DNA damage in cod larvae (Browman and Vetter, 2002). Importantly, spinal abnormalities and failure in formation of body axis during development are associated with the photo-enhanced toxicity of crude oil and PAHs on ELS of fish (Barron et al., 2003; Diamond et al., 2006; Farwell et al., 2006). Spinal abnormalities during development were also detected in UV-exposed zebrafish larvae (Torres Nuñez et al., 2012) and UVA-exposed medaka (*Oryzias latipes*) and African sharptooth catfish (*Clarias gariepinus*) embryos, where curvature of the notochord was observed (Mahmoud et al., 2009; Sayed and Mitani, 2016). Hence, the photo-enhanced effect of crude oil may lead to increased mortality and decreased growth and survival in nature as a result of spinal curvature deformities.

RNA-seq analysis revealed a higher number of DEGs in embryos co-exposed to crude oil and UV radiation (UV4 and UV5 groups) in comparison to embryos treated with only crude oil (N4 and N5). Several of the enriched pathways found in embryos from the UV4 and UV5 groups were also enriched in interaction analyses assessing the effect of the UV co-treatment on gene expression, indicating a photo-enhanced effect of crude oil. Circadian rhythm, oxidative stress and pathways related to mitochondrial function, the Nrf2 signaling pathway, tryptophan metabolism and retinoid metabolism were among these pathways and are discussed in more detail below.

4.4.1. Circadian rhythm pathway

Network analyses of up-regulated transcripts showed genes involved in circadian rhythm and DNA repair (Weger et al., 2011) in embryos from UV4 and UV5 groups, and some of them are related to the light responsive circadian rhythm pathway. Some of the light response pathways present in UV5 were also enriched in the UVC group. The circadian clock is regulated by light and controls physiological changes during the day-night cycle in most organisms (Reppert and Weaver,

Fig. 6. Quantitative polymerase chain reaction analyses (qPCR) of selected genes (A-L) in Atlantic cod (*Gadus morhua*) embryos. Expression of *ahr1a*, *ahr2a*, *cyp1a*, *ahrrb*, *cyp3a166* and *cyp24a1* was measured in Atlantic cod embryos 6 days post fertilization (dpf). Pool of 10 embryos ($n = 3$) were collected from each tank, but some samples were compromised during laboratory analysis. The data is presented as normalized log fold change values (points) and mean (cross). Statistical differences in log transformed fold change transcript levels between control and the different crude oil concentrations were assessed using a one-way ANOVA and Dunnet's multiple comparison tests in R v1.2.1335 software. Level of statistical significance is indicated with *($p < 0.05$), **($p < 0.01$) or ***($p < 0.001$).

2001). Induction of genes regulating circadian rhythm and DNA repair in embryos co-exposed to UV radiation is not surprising and is consistent with previous reports assessing genes and mechanisms involved in light regulation (Reppert and Weaver, 2001; Weger et al., 2011).

4.4.2. Oxidative stress

Many ROS-activated oxidative stress-related processes dominated the top pathways affected by photo-enhanced toxicity of crude-oil, as revealed by the interaction effect detected through transcriptome analysis. Mitochondrial iron dependent pathways, such as iron-sulfur cluster and heme synthesis (Horowitz and Greenamyre, 2011; Xu et al., 2013) were also affected as revealed in network analyses from UV4 and UV5 embryos. Additionally, some genes of the mitochondrial iron dependent pathways were part of the respiratory chain and ferroptosis pathways. Enrichment of the different mitochondrial pathways may suggest mitochondrial dysfunction in embryos from UV4 and UV5 groups, which is linked to impairment in mitochondrial respiration and subsequent shut-down of ATP production and mitochondria-dependent apoptosis (Ott et al., 2007; Simon et al., 2000). ROS are known to cause mitochondrial dysfunction by damaging important enzymes in the respiratory chain (Ott et al., 2007) or by affecting mitochondrial Ca^{2+} homeostasis (Ermak and Davies, 2001; Görlach et al., 2015). For instance, the disruption of Ca^{2+} balance between the sarcoplasmic/endoplasmic reticulum (SR/ER) and mitochondria has been described as an oxidative stress mechanism causing neuronal dysfunction and death in neurodegenerative diseases (Görlach et al., 2015; Guo et al., 2013). Another sign of mitochondrial dysfunction is the enrichment of the glycolysis and gluconeogenesis pathway in the N4 and N5 embryos. Upregulation of glycolysis is a compensatory mechanism that partially replaces ATP production when there is a mitochondrial dysfunction in an anaerobic manner (Lemasters et al., 1999). Ferroptosis pathway was also enriched in in UV4 and UV5 embryos, further indicating the existence of oxidative stress. Ferroptosis is an iron-dependent type of cell death driven by glutathione depletion, and subsequent production of lipid peroxides, ROS, and increase in intracellular Ca^{2+} levels (Lewerenz et al., 2018; Yang and Stockwell, 2016). Furthermore, important genes for mitochondrial Ca^{2+} transport were part of the ferroptosis pathway and up-regulated in co-exposed embryos from the UV5 group (Table 5). Mitochondrial dysfunction and apoptosis has also been associated with ROS production and oxidative stress in ELS of zebrafish (*Danio rerio*) (Jiang et al., 2019; Pan et al., 2018; Zhao et al., 2016) and fathead minnow (*Pimephales promelas*) (He et al., 2012) after exposure to environmental chemicals.

Activation of the Ahr pathway may have also contributed to an increased state of oxidative stress in embryos from UV4 and UV5 groups, since it has been demonstrated that AHR can induce production of ROS and oxidative stress by up-regulating the production of CYP enzymes (Dalton et al., 2002; Nebert et al., 2000). This mechanism is considered an important underlying cause of dioxin-induced toxicity and oxidative stress (Stohs, 1990). Recently, a role for AHR in modulating mitochondrial function has been described, where AHR disruption contributes to mitochondrial ROS production and mitochondrial dysfunction (Carreira et al., 2015; Senft et al., 2002; Tappenden et al., 2011).

Antioxidant responses were also observed in embryos from UV4 and UV5 groups, as suggested by the significant enrichment of the Nrf2 pathway. Upregulation of several genes involved in antioxidant responses was found in co-exposed embryos from the UV5 group (Table 5). Nrf2 has a major role in maintaining the redox cell homeostasis by mediating transcription of antioxidant enzymes, as well as proteins participating in detoxification of xenobiotics, such as glutathione S-transferases (GSTs) (Kensler et al., 2007; Nguyen et al., 2003; Ma, 2015). Antioxidant responses mediated by the Nrf2 pathway are important in skin for protection from UV radiation (Knatko et al., 2015; Marrot et al., 2007). The Nrf2 signaling pathway also mediates antioxidant responses in fish, where cellular oxidative stress responses elicited by cadmium exposure are Nrf2-mediated in zebrafish and in Jian carp (*Cyprinus carpio*) (Jiang et al., 2014; Wang and Gallagher, 2013). As reported in our study, Olsvik et al. observed an upregulation of different *gst* genes in cod larvae exposed to crude oil (Olsvik et al., 2010). Moreover, activation of the Ahr pathway might have also contributed to induction of antioxidant responses in embryos from UV4 and UV5 groups. A bidirectional cross-talk between AHR and Nrf2 appears to exist at the genetic level (Hayes et al., 2009; Miao et al., 2005; Shin et al., 2007), and it has proven to be necessary for induction of conjugating enzymes in mice exposed in vivo to TCDD (Yeager et al., 2009).

Even though gene regulation related to oxidative stress was observed in co-exposed embryos from UV4 and UV5 groups, oxidative stress may have also been induced in the N4 and N5 crude oil exposed groups through the Ahr pathway-mediated production of ROS. The state of increased oxidative stress may have led to cell death in the spinal cord and thus could be linked to the spinal curvature deformities observed in co-exposed cod larvae.

Our results are consistent with the well-studied mechanism of photoenhanced toxicity of PAHs in crude-oil through increased oxidative stress in aquatic organisms (Barron, 2017). PAH compounds excited by UV-radiation can transfer electrons to molecular oxygen and generate ROS (Barron, 2017; Barron et al., 2003). Increased ROS and reactive intermediates of photo-modified PAHs can react with cellular molecules causing DNA damage, lipid peroxidation and protein denaturation that increase cellular stress and damage (Yin et al., 2008). These increased oxidative stress processes have wide ranging consequences for cellular metabolism and survival and may explain many of the effects observed in the combined crude-oil and UV exposed larvae.

4.4.3. Tryptophan metabolism pathway

The tryptophan metabolism pathway was enriched in embryos from UVC, UV4 and UV5 groups. Tryptophan is a chromophore for UV light, and many of its photoproducts are endogenous AHR ligands (Denison and Nagy, 2003; Nguyen and Bradfield, 2008), including formylindolo [3, 2-b] carbazole (FICZ), which is one of the most potent AHR-ligand tryptophan derivatives. Induction of the AHR-mediated stress responses to UVB via transcriptional induction of *cyp1a* has been confirmed in vivo using AHR knockout mice (Fritsche et al., 2007). However, induction of the Ahr target gene *cyp1a* was not observed in embryos from the UVC group. On the other hand, *cyp1a* is a part of the tryptophan-enriched pathway revealed in UV4, UV5, and interaction analysis groups, suggesting a role of the Ahr signaling pathway in mediating UV responses in co-exposed cod embryos. Moreover, activation of the Ahr signaling pathway by FICZ occurs in zebrafish and cod with transcriptional induction of *cyp1a* (Aranguren-Abadía et al., 2020b; Jönsson et al., 2009).

4.4.4. Retinoid metabolism and vitamin D pathways

Pathway analysis suggested effects on retinol/vitamin A metabolism and signaling in co-exposed embryos from the UV4 and UV5 groups. Vitamin A and its metabolites are commonly referred to as retinoids. During embryogenesis, retinoids control a range of key events such as limb patterning, craniofacial and eye development (Ross et al., 2000). Disruption of retinoid metabolism and signaling have previously been observed in haddock following crude oil exposure during the embryonal and larval stages (Lie et al., 2019). Changes in gene expression and levels of key retinoids, were believed to be connected to the eye abnormalities observed in the same study. In the present study, the largest effects on vitamin A metabolism were observed in embryos from the UV5 group. Several of the genes related to vitamin A signaling previously reported to be affected by crude oil alone in haddock (*rdh10*, *rdh12*, *rarb*, *cyp3a* and *rpe6*), were also found in interaction analysis in the present study. The teratogenic properties of disrupted vitamin A metabolism cause developmental abnormalities in both fish and mammals (Colbert, 2002; Haga et al., 2002; Isken et al., 2008; Le et al., 2012; Lie et al., 2016), and the disruption of vitamin A signaling pathway could have contributed to the detrimental effects observed on co-exposed cod larvae from the UV4 and UV5 groups.

Disruption of vitamin A signaling has been observed following exposure to a range of chemicals (Benísek et al., 2008; Novák et al., 2008). Although the mechanisms are largely unclear and might vary depending on the properties of the individual contaminants, it has been hypothesized that increased Cyp induction leads to increased clearance of retinoids causing disruption of retinoid signaling in fish (Berntssen et al., 2015; Berntssen et al., 2016). Induction of the Ahr signaling pathway and *cyp1a* gene levels were similar between N4, N5, UV4, and UV5 groups, so a role of the Ahr in mediating the disruptions observed in the vitamin A pathway is not clear. Other molecular mechanisms possibly mediated by the photomodified PAHs formed after UV radiation exposure may explain alterations in the vitamin A pathway.

The vitamin D receptor (Vdr) target genes *cyp2r1* and *cyp24a1*, involved in the formation and clearance of the active form of vitamin D (calcitriol), respectively, were upregulated in co-exposed embryos from the UV5 group (Table 5, Table S7). Mammals synthesize vitamin D through UV-mediated photochemical conversion in the skin. Fish also have this ability, although this transformation is not likely to occur under natural conditions (Lock et al., 2010; Pierens and Fraser, 2015). Calcitriol is an important regulator of Ca^{2+} homeostasis and bone formation in fish (Lock et al., 2010; Sundell and Björnsson, 1990; Sundell et al., 1993). The CYP24A1 enzyme degrades and modulates excess calcitriol (Dzik and Kaczor, 2019; Jones et al., 2012), so an overexpression of *cyp24a1* may have led to vitamin D deficiency, affecting both Ca^{2+} homeostasis and bone formation in co-exposed cod larvae from the UV5 group.

Effects of environmental pollutants on modulating the Vdr signaling pathway have not been extensively studied in fish, but a cross-talk between AHR and VDR has been observed in human monocyte/macrophage-derived cells (Makishima, 2014; Matsunawa et al., 2012). AHR activation by benzo[*a*]pyrene enhanced calcitriol-dependent activation of VDR and induction of *Cyp24a1*, leading to inactivation of calcitriol, but the exact molecular mechanism responsible of this cross-talk is yet not known (Makishima, 2014; Matsunawa et al., 2009). Moreover, calcitriol enhanced benzo[*a*]pyrene-induced transcription of *Cyp1a1* through activation of VDR in different human cell lines, indicating a possible role of VDR in benzo[*a*]pyrene-mediated toxicity (Makishima, 2014; Matsunawa et al., 2012). In Atlantic cod, in vitro studies with Vdra and Vdrb have shown that some PAHs can interact with these receptors and modulate their activities (Goksøyr et al., 2021). Possible photooxidized PAHs may have induced the Vdr signaling pathway in co-exposed embryos from the UV5 group.

5. Conclusion

This study has provided insights into the mechanisms underlying developmental effects of crude oil in Atlantic cod. The study also provides important data on phenotypic outcomes and the underlying transcriptomic changes produced by the photo-enhanced toxicity of crude oil on ELS of Atlantic cod. Increased toxicity of crude oil in the presence of UV radiation was observed and may be the result of different mechanisms, such as enhanced oxidative stress. Our results are relevant to risk assessments that evaluate the putative effects of an oil spill on the ELS of Atlantic cod and the possible impact on cod stocks in important spawning areas.

Supplementary data to this article can be found online at https://doi.org/10.1016/j.scitotenv.2021.150697.

Funding

This work was supported by the Research Council of Norway (EGGTOX: *Unraveling the mechanistic effects of crude oil toxicity during early life stages of cold-water marine teleosts* (project no. 267820)), (*iCod 2.0: Integrative environmental genomics of Atlantic cod* (project no. 244564)), and the Center for Digital Life Norway (*dCod 1.0: decoding systems toxicology of Atlantic cod* (project no. 248840)).

CRediT authorship contribution statement

Libe Aranguren-Abadía: Investigation, Methodology, Formal analysis, Visualization, Writing – original draft. **Fekadu Yadetie:** Formal analysis, Visualization, Writing – review & editing. **Carey E. Donald:** Investigation, Visualization, Writing – review & editing. **Elin Sørhus:** Investigation, Formal analysis, Writing – review & editing. **Lars Eirik Myklatun:** Investigation. **Xiaokang Zhang:** Data curation, Formal analysis, Writing – review & editing. **Kai K. Lie:** Formal analysis, Writing – review & editing. **Prescilla Perrichon:** Investigation. **Charlotte L. Nakken:** Investigation, Formal analysis. **Caroline Durif:** Investigation. **Steven Shema:** Investigation. **Howard I. Browman:** Conceptualization, Methodology, Writing – review & editing. **Anne Berit Skiftesvik:** Methodology, Writing – review & editing. **Anders Goksøyr:** Funding acquisition, Writing – review & editing. **Sonnich Meier:** Conceptualization, Methodology, Investigation, Funding acquisition, Writing – review & editing, Supervision. **Odd André Karlsen:** Funding acquisition, Writing – review & editing, Supervision.

Declaration of competing interest

The authors declare that they have no known competing financial interests or personal relationships that could have appeared to influence the work reported in this paper.

Acknowledgments

We want to thank Margareth Møgster and Stig Ove Utskot, the technical staff of the Institute of Marine Research, Austevoll Aquaculture Research Station for their assistance and maintenance of the cod. We thank the Genomics Core Facility (GCF) at the Department of Clinical Science, University of Bergen, Norway for services rendered toward sequencing and analysis of genomic data and the Trond Mohn's Foundation for sponsoring these analysis. We also want to thank Pål Olsvik for helping with the analyses of the qPCR data, and Knut Helge Jensen for helping with statistical analysis.

References

Alloy, M., Baxter, D., Stieglitz, J., Mager, E., Hoenig, R., Benetti, D., Roberts, A., 2016. Ultraviolet radiation enhances the toxicity of Deepwater horizon oil to Mahi-mahi (Coryphaena hippurus) embryos. Environ. Sci. Technol. 50 (4), 2011–2017. https://doi.org/10.1021/acs.est.5b05356.

Ankley, G.T., Erickson, R.J., Sheedy, B.R., Kosian, P.A., Mattson, V.R., Cox, J.S., 1997. Evaluation of models for predicting the phototoxic potency of polycyclic aromatic hydrocarbons. Aquat. Toxicol. 37 (1), 37–50. https://doi.org/10.1016/S0166-445X(96)00803-X.

Aranguren-Abadía, L., Donald, C.E., Eilertsen, M., Gharbi, N., Tronci, V., Sørhus, E., Karlsen, O.A., 2020a. Expression and localization of the aryl hydrocarbon receptors and cytochrome P450 1A during early development of Atlantic cod (Gadus morhua). Aquat. Toxicol. 226 (June), 105558. https://doi.org/10.1016/j.aquatox.2020.105558.

Aranguren-Abadía, L., Lille-Langøy, R., Madsen, A.K., Karchner, S.I., Franks, D.G., Yadetie, F., Karlsen, O.A., 2020b. Molecular and functional properties of the Atlantic cod (Gadus morhua) aryl hydrocarbon receptors Ahr1a and Ahr2a. Environ. Sci. Technol. 54 (2), 1033–1044. https://doi.org/10.1021/acs.est.9b05312.

Arfsten, D.P., Schaeffer, D.J., Mulveny, D.C., 1996. The effects of near ultraviolet radiation on the toxic effects of polycyclic aromatic hydrocarbons in animals and plants: a review. Ecotoxicol. Environ. Saf. 33 (1), 1–24. https://doi.org/10.1006/eesa.1996.0001.

Barron, M.G., 2017. Photoenhanced toxicity of petroleum to aquatic invertebrates and fish. Arch. Environ. Contam. Toxicol. 73 (1), 40–46. https://doi.org/10.1007/s00244-016-0360-y.

Barron, M.G., Carls, M.G., Short, J.W., Rice, S.D., 2003. Photoenhanced toxicity of aqueous phase and chemically dispersed weathered Alaska north slope crude oil to Pacific herring eggs and larvae. Environ. Toxicol. Chem. 22 (3), 650–660. https://doi.org/10.1897/1551-5028(2003)022<0650:PTOAPA>2.0.CO;2.

Barron, M.G., Carls, M.G., Short, J.W., Rice, S.D., Heintz, R.A., Rau, M., Di Giulio, R., 2005. Assessment of the phototoxicity of weathered Alaska north slope crude oil to juvenile pink salmon. Chemosphere 60, 105–110. https://doi.org/10.1016/j.chemosphere.2004.12.006.

Barron, M.G., Krzykwa, J., Lilavois, C.R., Raimondo, S., 2018. Photoenhanced toxicity of weathered crude oil in sediment and water to larval zebrafish. Bull. Environ. Contam. Toxicol. 100 (1), 49–53. https://doi.org/10.1007/s00128-017-2228-x.

Barron, M.G., Vivian, D.N., Heintz, R.A., Yim, U.H., 2020. Long-term ecological impacts from oil spills: comparison of exxon valdez, hebei spirit, and deepwater horizon. Environ. Sci. Technol. 54 (11), 6456–6467. https://doi.org/10.1021/acs.est.9b05020.

Béland, F., Browman, H.I., Rodriguez, C.A., St-Pierre, J.F., 1999. Effect of solar ultraviolet radiation (280–400 nm) on the eggs and larvae of Atlantic cod (Gadus morhua). Can. J. Fish. Aquat. Sci. 56 (6), 1058–1067. https://doi.org/10.1139/f99-039.

Bence, A.E., Kvenvolden, K.A., Kennicutt, M.C., 1996. Organic geochemistry applied to environmental assessments of Prince William sound, Alaska, after the exxon Valdez oil spill - a review. Org. Geochem. 24 (1), 7–42. https://doi.org/10.1016/0146-6380(96)00010-1.

Benîšek, M., Bláha, L., Hilscherová, K., 2008. Interference of PAHs and their N-heterocyclic analogs with signaling of retinoids in vitro. Toxicol. in Vitro 22 (8), 1909–1917. https://doi.org/10.1016/j.tiv.2008.09.009.

Berdougo, E., Coleman, H., Lee, D.H., Stainier, D.Y.R., Yelon, D., 2003. Mutation of weak atrium/atrial myosin heavy chain disrupts atrial function and influences ventricular morphogenesis in zebrafish. Development 130 (24), 6121–6129. https://doi.org/10.1242/dev.00838.

Berntssen, M.H.G., Ørnsrud, R., Hamre, K., Lie, K.K., 2015. Polyaromatic hydrocarbons in aquafeeds, source, effects and potential implications for vitamin status of farmed fish species: a review. Aquac. Nutr. 21 (3), 257–273. https://doi.org/10.1111/anu.12309.

Berntssen, Marc H.G., Ørnsrud, R., Rasinger, J., Søfteland, L., Lock, E.J., Kolås, K., Lie, K., 2016. Dietary vitamin a supplementation ameliorates the effects of poly-aromatic hydrocarbons in Atlantic salmon (Salmo salar). Aquat. Toxicol. 175, 171–183. https://doi.org/10.1016/j.aquatox.2016.03.016.

Bertilsson, S., Widenfalk, A., 2002. Photochemical degradation of PAHs in freshwaters and their impact on bacterial growth - influence of water chemistry. Hydrobiologia 469, 23–32. https://doi.org/10.1023/A:1015579628189.

Beyer, J., Sandvik, M., Hylland, K., Fjeld, E., Egaas, E., Aas, E., Goksøyr, A., 1996. Contaminant accumulation and biomarker responses in flounder (Platichthys flesus L.) and Atlantic cod (Gadus morhua L.) exposed by caging to polluted sediments in Sørfjorden, Norway. Aquat. Toxicol. 36 (1–2), 75–98. https://doi.org/10.1016/S0166-445X(96)00798-9.

Bjørkan, M., Veland, S., 2019. Beyond concensus: perceptions of risk from petroleum developments in Lofoten, Vesterålen, and Senja, Norway. ICES J. Mar. Sci. 76 (6), 1935. https://doi.org/10.1093/icesjms/fsz096.

Boehm, P.D., Neff, J.M., Page, D.S., 2007. Assessment of polycyclic aromatic hydrocarbon exposure in the waters of Prince William sound after the exxon Valdez oil spill: 1989–2005. Mar. Pollut. Bull. 54 (3), 339–356. https://doi.org/10.1016/j.marpolbul.2006.11.025.

Boehm, P.D., Murray, K.J., Cook, L.L., 2016. Distribution and attenuation of polycyclic aromatic hydrocarbons in Gulf of Mexico seawater from the Deepwater horizon oil accident. Environ. Sci. Technol. 50 (2), 584–592. https://doi.org/10.1021/acs.est.5b03616.

Brette, F., Machado, B., Cros, C., Incardona, J.P., Scholz, N.L., Block, B.A., 2014. Crude oil impairs cardiac excitation-contraction coupling in fish. Science 343 (6172), 772–776. https://doi.org/10.1126/science.1242747.

Brette, F., Shiels, H.A., Galli, G.L.J., Cros, C., Incardona, J.P., Scholz, N.L., Block, B.A., 2017. A novel cardiotoxic mechanism for a pervasive global pollutant. Sci. Rep. 7, 1–9. https://doi.org/10.1038/srep41476.

Browman, H.I., Vetter, R.D., 2002. Impacts of ultraviolet radiation on crustacean zooplankton and ichthyoplankton: case studies from subarctic marine ecosystems. Ecological Studies. Vol. 153, pp. 261–304. https://doi.org/10.1007/978-3-642-56075-0_13.

Carls, M.G., Meador, J.P., 2009. A perspective on the toxicity of petrogenic pahs to developing fish embryos related to environmental chemistry. Hum. Ecol. Risk. Assess. 15 (6), 1084–1098. https://doi.org/10.1080/10807030903304708.

Carls, M.G., Rice, S.D., Hose, J.E., 1999. Sensitivity of fish embryos to weathered crude oil: part I. Low-level exposure during incubation causes malformations, genetic damage, and mortality in larval pacific herring (Clupea pallasi). Environ. Toxicol. Chem. 18 (3), 481–493. https://doi.org/10.1897/1551-5028(1999)018<0481:SOFETW>2.3.CO;2.

Carreira, V.S., Fan, Y., Wang, Q., Zhang, X., Kurita, H., Ko, C.-I., Puga, A., 2015. Ah receptor signaling controls the expression of cardiac development and homeostasis genes. Toxicol. Sci. 147 (2), 425–435. https://doi.org/10.1093/toxsci/kfv138.

Celander, M.C., 2011. Cocktail effects on biomarker responses in fish. Aquat. Toxicol. 105 (3–4 SUPPL.), 72–77. https://doi.org/10.1016/j.aquatox.2011.06.002.

Chang, C.T., Chung, H.Y., Su, H.T., Tseng, H.P., Tzou, W.S., Hu, C.H., 2013. Regulation of zebrafish CYP3A65 transcription by AHR2. Toxicol. Appl. Pharmacol. 270 (2), 174–184. https://doi.org/10.1016/j.taap.2013.04.010.

Chen, E.Y., Tan, C.M., Kou, Y., Duan, Q., Wang, Z., Meirelles, G.V., Maayan, A., 2013. Enrichr: interactive and collaborative HTML5 gene list enrichment analysis tool. BMC Bioinf. 14 (128), 1–14. https://doi.org/10.1007/s00701-014-2321-4.

Cherr, G.N., Fairbairn, E., Whitehead, A., 2017. Impacts of petroleum-derived pollutants on fish development. Annu. Rev. Anim. Biosci. 5 (1), 185–203. https://doi.org/10.1146/annurev-animal-022516-022928.

Chomczynski, P., 1993. A reagent for the single-step simultaneous isolation of RNA, DNA and proteins from cell and tissue samples. Biotechniques 15 (3) 532-4,536-7.

Clark, B.W., Matson, C.W., Jung, D., Di Giulio, R.T., 2010. AHR2 mediates cardiac teratogenesis of polycyclic aromatic hydrocarbons and PCB-126 in Atlantic killifish (Fundulus heteroclitus). Aquat. Toxicol. 99 (2), 232–240. https://doi.org/10.1016/j.aquatox.2010.05.004.

Coffin Talbot, J., Johnson, S.L., Kimmel, C.B., 2010. hand2 and dlx genes specify dorsal, intermediate and ventral domains within zebrafish pharyngeal arches. Development 137 (15), 2507–2517. https://doi.org/10.1242/dev.049700.

Colavecchia, M.V., Backus, S.M., Hodson, P.V., Parrott, J.L., 2004. Toxicity of oil sands to early life stages of fathead minnows (Pimephales promelas). Environ. Toxicol. Chem. 23 (7), 1709–1718. https://doi.org/10.1897/03-412.

Colavecchia, M., Hodson, P., Parrott, J., 2006. CYP1A induction and blue sac disease in early life stages of white suckers (Catostomus commersoni) exposed to oil sands. J. Toxicol. Environ. Health, Part A 69 (10), 967–994. https://doi.org/10.1080/15287390500362154.

Colbert, M.C., 2002. Retinoids and cardiovascular developmental defects. Cardiovasc. Toxicol. 2 (1), 25–39. https://doi.org/10.1385/CT:2:1:25.

Crawley, M.J., 2012. The R Book (Second). Wiley, New York.

Cunha, V., Vogs, C., Le Bihanic, F., Dreij, K., 2020. Mixture effects of oxygenated PAHs and benzo[a]pyrene on cardiovascular development and function in zebrafish embryos. Environ. Int. 143 (April), 105913. https://doi.org/10.1016/j.envint.2020.105913.

Dale, K., Müller, M.B., Tairova, Z., Khan, E.A., Hatlen, K., Grung, M., Goksøyr, A., 2019. Contaminant accumulation and biological responses in Atlantic cod (Gadus morhua) caged at a capped waste disposal site in Kollevåg, Western Norway. Mar. Environ. Res. 145, 39–51. https://doi.org/10.1016/j.marenvres.2019.02.003.

Dalton, T.P., Puga, A., Shertzer, H.G., 2002. Induction of cellular oxidative stress by aryl hydrocarbon receptor activation. Chem. Biol. Interact. 141 (1–2), 77–95. https://doi.org/10.1016/S0009-2797(02)00067-4.

Denison, M.S., Nagy, S.R., 2003. Activation of the aryl hydrocarbon receptor by structurally diverse exogenous and endogenous chemicals. Annu. Rev. Pharmacol. Toxicol. 43 (1), 309–334. https://doi.org/10.1146/annurev.pharmtox.43.100901.135828.

Denison, M.S., Soshilov, A.A., He, G., Degroot, D.E., Zhao, B., 2011. Exactly the same but different : promiscuity and diversity in the molecular mechanisms of action of the aryl hydrocarbon (dioxin) receptor. Toxicol. Sci. 124 (1), 1–22. https://doi.org/10.1093/toxsci/kfr218.

Diamond, S.A., Mount, D.R., Mattson, V.R., Heinis, L.J., Highland, T.L., Adams, A.D., Simcik, M.F., 2006. Photoactivated polycyclic aromatic hydrocarbon toxicity in medaka (Oryzias latipes) embryos: relevance to environmental risk in contaminated sites. Environ. Toxicol. Chem. 25 (11), 3015–3023. https://doi.org/10.1897/06-038R.1.

Dzik, K.P., Kaczor, J.J., 2019. Mechanisms of vitamin D on skeletal muscle function: oxidative stress, energy metabolism and anabolic state. Eur. J. Appl. Physiol. 119 (4), 825–839. https://doi.org/10.1007/s00421-019-04104-x.

Eide, M., Rydbeck, H., Tørresen, O.K., Lille-Langøy, R., Puntervoll, P., Goldstone, J.V., Karlsen, O.A., 2018. Independent losses of a xenobiotic receptor across teleost evolution. Sci. Rep. 8 (1), 1–13. https://doi.org/10.1038/s41598-018-28498-4.

Ermak, G., Davies, K.J.A., 2001. Calcium and oxidative stress: from cell signaling to cell death. Mol. Immunol. 38 (10), 713–721. https://doi.org/10.1016/S0161-5890(01)00108-0.

Farwell, A.J., Nero, V., Croft, M., Rhodes, S., Dixon, D.G., 2006. Phototoxicity of oil sands-derived polycyclic aromatic compounds to japanese medaka (Oryzias latipes) embryos. Environ. Toxicol. Chem. 25 (12), 3266–3274. https://doi.org/10.1897/05-637R1.1.

Fritsche, E., Schäfer, C., Calles, C., Bernsmann, T., Bernshausen, T., Wurm, M., Krutmann, J., 2007. Lightening up the UV response by identification of the arylhydrocarbon receptor as a cytoplasmatic target for ultraviolet B radiation. Proc. Natl. Acad. Sci. U. S. A. 104 (21), 8851–8856. https://doi.org/10.1073/pnas.0701764104.

Glickman, N.S., Yelon, D., 2002. Cardiac development in zebrafish: coordination of form and function. Semin. Cell Dev. Biol. 13, 507–513. https://doi.org/10.1016/S1084952102001040.

Goksøyr, A., 1995. Use of cytochrome P450 1A (CYP1A) in fish as a biomarker of aquatic pollution. In: Degen, G.H., Seiler, J.P., Bentley, P. (Eds.), Toxicology in Transition: Proceedings of the 1994 EUROTOX Congress Meeting Held in Basel, Switzerland, August 21–24, 1994, pp. 80–95 https://doi.org/10.1007/978-3-642-79451-3_7.

Goksøyr, A., Förlin, L., 1992a. The cytochrome P-450 system in fish, aquatic toxicology and environmental monitoring. Aquat. Toxicol. 22 (4), 287–311. https://doi.org/10.1016/0166-445X(92)90046-P.

Goksøyr, A., Förlin, L., 1992b. The cytochrome P-450 system in fish, aquatic toxicology and environmental monitoring. Aquat. Toxicol. https://doi.org/10.1016/0166-445X(92)90046-P.

Goksøyr, A., Solberg, T.S., Serigstad, B., 1991. Immunochemical detection fo cytrochrome P450lA1 induction in cod larvae and juveniles exposed to a water soluble fraction of North Sea crude oil. Mar. Pollut. Bull. 22 (3), 122–127.

Goksøyr, A., Beyer, J., Husøy, A.M., Larsen, H.E., Westrheim, K., Wilhelmsen, S., Klungsøyr, J., 1994. Accumulation and effects of aromatic and chlorinated hydrocarbons in juvenile Atlantic cod (Gadus morhua) caged in a polluted fjord (Sørfjorden, Norway). Aquat. Toxicol. 29, 21–35. https://doi.org/10.1016/0166-445X(94)90045-0.

Goksøyr, S.Ø., Goldstone, J., Lille-Langøy, R., Lock, E.J., Olsvik, P.A., Goksøyr, A., Karlsen, O.A., 2021. Polycyclic aromatic hydrocarbons modulate the activity of Atlantic cod (Gadus morhua) vitamin D receptor paralogs in vitro. Aquat. Toxicol. 238 (July). https://doi.org/10.1016/j.aquatox.2021.105914.

Görlach, A., Bertram, K., Hudecova, S., Krizanova, O., 2015. Calcium and ROS: a mutual interplay. Redox Biol. 6, 260–271. https://doi.org/10.1016/j.redox.2015.08.010.

Guo, C., Sun, L., Chen, X., Zhang, D., 2013. Oxidative stress, mitochondrial damage and neurodegenerative diseases. Neural Regen. Res. 8 (21), 2003–2014. https://doi.org/10.3969/j.issn.1673-5374.2013.21.009.

Haga, Y., Takeuchi, T., Seikai, T., 2002. Influence of all-trans retinoic acid on pigmentation and skeletal formation in larval japanese flounder. Fish. Sci. 68 (3), 560–570. https://doi.org/10.1046/j.1444-2906.2002.00462.x.

Hall, T.E., Smith, P., Johnston, I.A., 2004. Stages of embryonic development in the Atlantic cod Gadus morhua. J. Morphol. 259 (3), 255–270. https://doi.org/10.1002/jmor.10222.

Hatlen, K., Sloan, C.A., Burrows, D.G., Collier, T.K., Scholz, N.L., Incardona, J.P., 2010. Natural sunlight and residual fuel oils are an acutely lethal combination for fish embryos. Aquat. Toxicol. 99, 56–64. https://doi.org/10.1016/j.aquatox.2010.04.002.

Hayes, J.D., Dinkova-Kostova, A.T., Mcmahon, M., 2009. Cross-talk between transcription factors AhR and Nrf2: lessons for cancer chemoprevention from dioxin. Toxicol. Sci. 111 (2), 199–201. https://doi.org/10.1093/toxsci/kfp168.

He, Y., Patterson, S., Wang, N., Hecker, M., Martin, J.W., El-Din, M.G., Wiseman, S.B., 2012. Toxicity of untreated and ozone-treated oil sands process-affected water (OSPW) to early life stages of the fathead minnow (Pimephales promelas). Water Res. 46 (19), 6359–6368. https://doi.org/10.1016/j.watres.2012.09.004.

Hodson, P.V., 2017. The toxicity to fish embryos of PAH in crude and refined oils. Arch. Environ. Contam. Toxicol. 73 (1), 12–18. https://doi.org/10.1007/s00244-016-0357-6.

Holth, T.F., Eidsvoll, D.P., Farmen, E., Sanders, M.B., Martínez-Gómez, C., Budzinski, H., Hylland, K., 2014. Effects of water accommodated fractions of crude oils and diesel on a suite of biomarkers in Atlantic cod (Gadus morhua). Aquat. Toxicol. 154, 240–252. https://doi.org/10.1016/j.aquatox.2014.05.013.

Honrath, B., Metz, I., Bendridi, N., Rieusset, J., Culmsee, C., Dolga, A.M., 2017. Glucose-regulated protein 75 determines ER–mitochondrial coupling and sensitivity to oxidative stress in neuronal cells. Cell Death Discovery 3 (1), 1–13. https://doi.org/10.1038/cddiscovery.2017.76.

Horowitz, M.P., Greenamyre, T., 2011. Mito iron metabolism and neurodegeneration. J. Alzheimers Dis. 20 (Suppl. 2), 1–25. https://doi.org/10.3233/JAD-2010-100354.Mitochondrial.

Husøy, A.-M., Myers, M.S., Goksøyr, A., 1996. Cellular localization of cytochrome P450 (CYPl A) induction and histology in Atlantic cod (Gadus morhua L.) and European flounder (Platichthys flesus) after environmental exposure to contaminants by caging in Sarrfiorden, Norway. Aquat. Toxicol. 36, 53–74.

Hylland, K., Tollefsen, K.E., Ruus, A., Jonsson, G., Sundt, R.C., Sanni, S., Børseth, J.F., 2008. Water column monitoring near oil installations in the North Sea 2001–2004. Mar. Pollut. Bull. 56 (3), 414–429. https://doi.org/10.1016/j.marpolbul.2007.11.004.

Incardona, J.P., 2017. Molecular mechanisms of crude oil developmental toxicity in fish. Arch. Environ. Contam. Toxicol. 73 (1), 19–32. https://doi.org/10.1007/s00244-017-0381-1.

Incardona, J.P., Collier, T.K., Scholz, N.L., 2004. Defects in cardiac function precede morphological abnormalities in fish embryos exposed to polycyclic aromatic hydrocarbons. Toxicol. Appl. Pharmacol. 196 (2), 191–205. https://doi.org/10.1016/j.taap.2003.11.026.

Incardona, J.P., Day, H.L., Collier, T.K., Scholz, N.L., 2006. Developmental toxicity of 4-ring polycyclic aromatic hydrocarbons in zebrafish is differentially dependent on AH receptor isoforms and hepatic cytochrome P4501A metabolism. Toxicol. Appl. Pharmacol. 217, 308–321. https://doi.org/10.1016/j.taap.2006.09.018.

Incardona, J.P., Linbo, T.L., Scholz, N.L., 2011. Cardiac toxicity of 5-ring polycyclic aromatic hydrocarbons is differentially dependent on the aryl hydrocarbon receptor 2 isoform during zebrafish development. Toxicol. Appl. Pharmacol. 257, 242–249. https://doi.org/10.1016/j.taap.2011.09.010.

Incardona, J.P., Vines, C.A., Linbo, T.L., Myers, M.S., Sloan, C.A., Anulacion, B.F., Scholz, N.L., 2012. Potent phototoxicity of marine bunker oil to translucent herring embryos after prolonged weathering. PLoS One 7 (2). https://doi.org/10.1371/journal.pone.0030116.

Isken, A., Golczak, M., Oberhauser, V., Hunzelmann, S., Driever, W., Imanishi, Y., von Lintig, J., 2008. RBP4 disrupts vitamin a uptake homeostasis in a STRA6-deficient animal model for Matthew-wood syndrome. Cell Metab. 7 (3), 258–268. https://doi.org/10.1016/j.cmet.2008.01.009.

Jiang, W.D., Liu, Y., Hu, K., Jiang, J., Li, S.H., Feng, L., Zhou, X.Q., 2014. Copper exposure induces oxidative injury, disturbs the antioxidant system and changes the Nrf2/ARE (CuZnSOD) signaling in the fish brain: protective effects of myo-inositol. Aquat. Toxicol. 155 (46), 301–313. https://doi.org/10.1016/j.aquatox.2014.07.003.

Jiang, J., Wu, S., Lv, L., Liu, X., Chen, L., Zhao, X., Wang, Q., 2019. Mitochondrial dysfunction, apoptosis and transcriptomic alterations induced by four strobilurins in zebrafish (Danio rerio) early life stages. Environ. Pollut. 253, 722–730. https://doi.org/10.1016/j.envpol.2019.07.081.

Jones, G., Prosser, D.E., Kaufmann, M., 2012. 25-hydroxyvitamin D-24-hydroxylase (CYP24A1): its important role in the degradation of vitamin D. Arch. Biochem. Biophys. 523 (1), 9–18. https://doi.org/10.1016/j.abb.2011.11.003.

Jönsson, M.E., Franks, D.G., Woodin, B.R., Jenny, M.J., Garrick, R.A., Behrendt, L., Stegeman, J.J., 2009. The tryptophan photoproduct 6-formylindolo[3,2-b]carbazole (FICZ) binds multiple AHRs and induces multiple CYP1 genes via AHR2 in zebrafish. Chem. Biol. Interact. 181 (3), 447–454. https://doi.org/10.1016/j.cbi.2009.07.003.

Kensler, T.W., Wakabayashi, N., Biswal, S., 2007. Cell survival responses to environmental stresses via the Keap1-Nrf2-ARE pathway. Annu. Rev. Pharmacol. Toxicol. 47 (1), 89–116. https://doi.org/10.1146/annurev.pharmtox.46.120604.141046.

Kim, D., Langmead, B., Salzberg, S.L., 2015. HISAT: a fast spliced aligner with low memory requirements. Nat. Methods 12, 357–360.

Kim, D., Paggi, J.M., Park, C., Bennett, C., Salzberg, S.L., 2019. Graph-based genome alignment and genotyping with HISAT2 and HISAT-genotype. Nat. Biotechnol. 37 (8), 907–915. https://doi.org/10.1038/s41587-019-0201-4.

Knatko, E.V., Ibbotson, S.H., Zhang, Y., Higgins, M., Fahey, J.W., Talalay, P., Dinkova-Kostova, A.T., 2015. Nrf2 activation protects against solar-simulated ultraviolet radiation in mice and humans. Cancer Prev. Res. 8 (6), 475–486. https://doi.org/10.1158/1940-6207.CAPR-14-0362.

Kouwenberg, J.H.M., Browman, H.I., St-Pierre, J.F., Runge, J.A., Cullen, J.J., Davis, R.F., 1999. Biological weighting of ultraviolet (280–400 nm) induced mortality in marine zooplankton and fish. I. Atlantic cod (Gadus morhua) eggs. Mar. Biol. 134 (2), 269–284. https://doi.org/10.1007/s002270050545.

Kubota, A., Goldstone, J.V., Lemaire, B., Takata, M., Woodin, B.R., Stegeman, J.J., 2015. Role of pregnane X receptor and aryl hydrocarbon receptor in transcriptional regulation of pxr, CYP2, and CYP3 genes in developing zebrafish. Toxicol. Sci. 143 (2), 398–407. https://doi.org/10.1093/toxsci/kfu240.

Kuleshov, M.V., Jones, M.R., Rouillard, A.D., Fernandez, N.F., Duan, Q., Wang, Z., Ma'ayan, A., 2016. Enrichr: a comprehensive gene set enrichment analysis web server 2016 update. Nucleic Acids Res. 44 (W1), W90–W97. https://doi.org/10.1093/nar/gkw377.

Lanham, K.A., Plavicki, J., Peterson, R.E., Heideman, W., 2014. Cardiac myocyte-specific ahr activation phenocopies tcdd-induced toxicity in zebrafish. Toxicol. Sci. 141 (1), 141–154. https://doi.org/10.1093/toxsci/kfu111.

Le, H.G.T., Dowling, J.E., Cameron, D.J., 2012. Early retinoic acid deprivation in developing zebrafish results in microphthalmia. Vis. Neurosci. 29 (4–5), 219–228. https://doi.org/10.1017/S0952523812000296.

Lemasters, J.J., Qian, T., Bradham, C.A., Brenner, D.A., Cascio, W.E., Trost, L.C., Herman, B., 1999. Mitochondrial dysfunction in the pathogenesis of necrotic and apoptotic cell death. J. Bioenerg. Biomembr. 31 (4), 305–319. https://doi.org/10.1023/A:1005419617371.

Lesser, M.P., Farrell, J.H., Walker, C.W., 2001. Oxidative stress, DNA damage and p53 expression in the larvae of Atlantic cod (Gadus morhua) exposed to ultraviolet (290–400 nm) radiation. J. Exp. Biol. 204 (1), 157–164.

Lewerenz, J., Ates, G., Methner, A., Conrad, M., Maher, P., 2018. Oxytosis/ferroptosis-(Re-) emerging roles for oxidative stress-dependent non-apoptotic cell death in diseases of the central nervous system. Front. Neurosci. 12 (APR). https://doi.org/10.3389/fnins.2018.00214.

Liao, Y., Smyth, G.K., Shi, W., 2014. FeatureCounts: an efficient general purpose program for assigning sequence reads to genomic features. Bioinformatics 30 (7), 923–930. https://doi.org/10.1093/bioinformatics/btt656.

Lie, Kai Kristoffer, Kvalheim, K., Rasinger, J.D., Harboe, T., Nordgreen, A., Moren, M., 2016. Vitamin a and arachidonic acid altered the skeletal mineralization in Atlantic cod (Gadus morhua) larvae without any interactions on the transcriptional level. Comp. Biochem. Physiol. A Mol. Integr. Physiol. 191, 80–88. https://doi.org/10.1016/j.cbpa.2015.10.011.

Lie, Kai K., Meier, S., Sørhus, E., Edvardsen, R.B., Karlsen, Ø., Olsvik, P.A., 2019. Offshore crude oil disrupts retinoid signaling and eye development in larval Atlantic haddock. Front. Mar. Sci. 6 (JUL), 1–14. https://doi.org/10.3389/fmars.2019.00368 532-4,536-7.

Little, E.E., Cleveland, L., Calfee, R., Barron, M.G., 2000. Assessment of the photoenhanced toxicity of a weathered oil to the tidewater silverside. Environ. Toxicol. Chem. 19 (4 I), 926–932. https://doi.org/10.1002/etc.5620190420.

Lock, E.J., WaagbØ, R., Wendelaar Bonga, S., Flik, G., 2010. The significance of vitamin D for fish: a review. Aquac. Nutr. 16 (1), 100–116. https://doi.org/10.1111/j.1365-2095.2009.00722.x.

Ma, Qiang, 2015. Role of Nrf2 in oxidative stress and toxicity. Annu. Rev. Pharmacol. Toxicol. 1, 401–426. https://doi.org/10.1146/annurev-pharmtox-011112-140320.Role.

Mahmoud, U.M., Mekkawy, I.A.A., Sayed, A.E.D.H., 2009. Ultraviolet radiation-a (366 nm) induced morphological and histological malformations during embryogenesis of Clarias gariepinus (Burchell, 1822). J. Photochem. Photobiol. B Biol. 95, 117–128. https://doi.org/10.1016/j.jphotobiol.2009.02.003.

Maki, H., Sasaki, T., Harayama, S., 2001. Photo-oxidation of biodegraded crude oil and toxicity of the photo-oxidized products. Chemosphere 44 (5), 1145–1151. https://doi.org/10.1016/S0045-6535(00)00292-7.

Makishima, M., 2014. Cooperative regulation of expression of cytochrome P450 enzymes by aryl hydrocarbon receptor and vitamin D receptor. In: Yamazaki, H. (Ed.), Fifty Years of Cytochrome P450 Research, pp. 277–290 https://doi.org/10.1007/978-4-431-54992-5_16.

Marrot, L., Jones, C., Perez, P., Meunier, J.R., 2007. The significance of Nrf2 pathway in (photo)-oxidative stress response in melanocytes and keratinocytes of the human epidermis. Pigment Cell Melanoma Res. 21 (1), 79–88. https://doi.org/10.1111/j.1755-148X.2007.00424.x.

Marty, G.D., Hose, J.E., McGurk, M.D., Brown, E.D., Hinton, D.E., 1997. Histopathology and cytogenetic evaluation of Pacific herring larvae exposed to petroleum hydrocarbons in the laboratory or in Prince William sound, Alaska, after the exxon Valdez oil spill. Can. J. Fish. Aquat. Sci. 54 (8), 1846–1857. https://doi.org/10.1139/f97-091.

Matsunawa, M., Amano, Y., Endo, K., Uno, S., Sakaki, T., Yamada, S., Makishima, M., 2009. The aryl hydrocarbon receptor activator benzo[a]pyrene enhances vitamin D3 catabolism in macrophages. Toxicol. Sci. 109 (1), 50–58. https://doi.org/10.1093/toxsci/kfp044.

Matsunawa, M., Akagi, D., Uno, S., Endo-Umeda, K., Yamada, S., Ikeda, K., Makishima, M., 2012. Vitamin D receptor activation enhances benzo[a]pyrene metabolism via CYP1A1 expression in macrophages. Drug Metab. Dispos. 40 (11), 2059–2066. https://doi.org/10.1124/dmd.112.046839.

McCarthy, D.J., Chen, Y., Smyth, G.K., 2012. Differential expression analysis of multifactor RNA-seq experiments with respect to biological variation. Nucleic Acids Res. 40 (10), 4288–4297. https://doi.org/10.1093/nar/gks042.

Meador, J.P., Nahrgang, J., 2019. Characterizing crude oil toxicity to early-life stage fish based on a complex mixture: are we making unsupported assumptions? Environ. Sci. Technol. 53 (19), 11080–11092. https://doi.org/10.1021/acs.est.9b02889.

Meier, S., Morton, H.C., Nyhammer, G., Grøsvik, B.E., Makhotin, V., Geffen, A., Svardal, A., 2010. Development of Atlantic cod (Gadus morhua) exposed to produced water during early life stages: effects on embryos, larvae, and juvenile fish. Mar. Environ. Res. 70 (5), 383–394. https://doi.org/10.1016/j.marenvres.2010.08.002.

Miao, W., Hu, L., Scrivens, P.J., Batist, G., 2005. Transcriptional regulation of NF-E2 p45-related factor (NRF2) expression by the aryl hydrocarbon receptor-xenobiotic response element signaling pathway: direct cross-talk between phase I and II drug-metabolizing enzymes. J. Biol. Chem. 280 (21), 20340–20348. https://doi.org/10.1074/jbc.M412081200.

Misund, O.A., Olsen, E., 2013. Lofoten-Vesterålen: for cod and cod fisheries, but not for oil? ICES J. Mar. Sci. 70 (4), 722–725. https://doi.org/10.1038/278097a0.

Nebert, D.W., 2017. Aryl hydrocarbon receptor (AHR): "pioneer member" of the basic-helix/loop/helix per-arnt-Sim (bHLH/PAS) family of "sensors" of foreign and endogenous signals. Prog. Lipid Res. 67 (June), 38–57. https://doi.org/10.1016/j.plipres.2017.06.001.

Nebert, D.W., Roe, A.L., Dieter, M.Z., Solis, W.A., Yang, Y., Dalton, T.P., 2000. Role of the aromatic hydrocarbon receptor and (Ah) gene battery in the oxidative stress response, cell cycle control, and apoptosis. Biochem. Pharmacol. 59 (1), 65–85. https://doi.org/10.1016/S0006-2952(99)00310-X.

Nguyen, L.P., Bradfield, C.A., 2008. The search for endogenous activators of the aryl hydrocarbon receptor. Chem. Res. Toxicol. 21, 102–116.

Nguyen, T., Sherratt, P.J., Pickett, C.B., 2003. Regulatory mechanisms controlling gene expression mediated by the antioxidant response element. Annu. Rev. Pharmacol. Toxicol. 43 (2), 233–260. https://doi.org/10.1146/annurev.pharmtox.43.100901.140229.

Nilsen, B.M., Berg, K., Goksøyr, A., 1998. Induction of cytochrome P4501A (CYP1A) in fish a biomarker for environmental pollution. In: Phillips, I.R., Shephard, E.A. (Eds.), Cytochrome P450 Protocols, pp. 423–438 https://doi.org/10.1385/0-89603-519-0:423.

Nordtug, T., Olsen, A.J., Altin, D., Meier, S., Overrein, I., Hansen, B.H., Johansen, Ø., 2011. Method for generating parameterized ecotoxicity data of dispersed oil for use in environmental modelling. Mar. Pollut. Bull. 62 (10), 2106–2113. https://doi.org/10.1016/j.marpolbul.2011.07.015.

Novák, J., Beníšek, M., Hilscherová, K., 2008. Disruption of retinoid transport, metabolism and signaling by environmental pollutants. Environ. Int. 34 (6), 898–913. https://doi.org/10.1016/j.envint.2007.12.024.

Okey, A.B., 2007. An aryl hydrocarbon receptor odyssey to the shores of toxicology: the Deichmann Lecture, International Congress of Toxicology-XI. Toxicol. Sci. 98 (1), 5–38. https://doi.org/10.1093/toxsci/kfm096.

Olsen, E., Aanes, S., Mehl, S., Holst, J.C., Aglen, A., Gjøsæter, H., 2009. Cod, haddock, saithe, herring, and capelin in the Barents Sea and adjacent waters: a review of the biological value of the area. ICES J. Mar. Sci. 67 (1), 87–101. https://doi.org/10.1093/icesjms/fsp229.

Olsvik, Pål A., Søfteland, L., Lie, K.K., 2008. Selection of reference genes for qRT-PCR examination of wild populations of Atlantic cod Gadus morhua. BMC Res. Notes 1, 1–9. https://doi.org/10.1186/1756-0500-1-47.

Olsvik, P.A., Nordtug, T., Altin, D., Lie, K.K., Overrein, I., Hansen, B.H., 2010. Transcriptional effects on glutathione S-transferases in first feeding Atlantic cod (Gadus morhua) larvae exposed to crude oil. Chemosphere 79 (9), 905–913. https://doi.org/10.1016/j.chemosphere.2010.03.026.

OSPAR, 2010. Background Document for Atlantic cod Gadus morhua London.

Ott, M., Gogvadze, V., Orrenius, S., Zhivotovsky, B., 2007. Mitochondria, oxidative stress and cell death. Apoptosis 12 (5), 913–922. https://doi.org/10.1007/s10495-007-0756-2.

Pan, Y.X., Luo, Z., Zhuo, M.Q., Wei, C.C., Chen, G.H., Song, Y.F., 2018. Oxidative stress and mitochondrial dysfunction mediated cd-induced hepatic lipid accumulation in zebrafish Danio rerio. Aquat. Toxicol. 199 (March), 12–20. https://doi.org/10.1016/j.aquatox.2018.03.017.

Perrichon, P., Mager, E.M., Pasparakis, C., Stieglitz, J.D., Benetti, D.D., Grosell, M., Burggren, W.W., 2018. Combined effects of elevated temperature and Deepwater Horizon oil exposure on the cardiac performance of larval mahi-mahi, Coryphaena hippurus. PLoS One 13 (10), 1–19. https://doi.org/10.1371/journal.pone.0203949.

Pierens, S.L., Fraser, D.R., 2015. The origin and metabolism of vitamin D in rainbow trout. J. Steroid Biochem. Mol. Biol. 145, 58–64. https://doi.org/10.1016/j.jsbmb.2014.10.005.

Planchart, A., Mattingly, C.J., 2010. 2,3,7,8-tetrachlorodibenzo-P-dioxin upregulates Foxq1B in zebrafish jaw primordium. Chem. Res. Toxicol. 23 (3), 480–487. https://doi.org/10.1021/tx9003165.

Pollino, C.A., Holdway, D.A., 2002. Toxicity testing of crude oil and related compounds using early life stages of the crimson-spotted rainbowfish (Melanotaenia fluviatilis). Ecotoxicol. Environ. Saf. 52 (3), 180–189. https://doi.org/10.1006/eesa.2002.2190.

Ray, P.Z., Chen, H., Podgorski, D.C., McKenna, A.M., Tarr, M.A., 2014. Sunlight creates oxygenated species in water-soluble fractions of Deepwater horizon oil. J. Hazard. Mater. 280, 636–643. https://doi.org/10.1016/j.jhazmat.2014.08.059.

Reiter, J.F., Verkade, H., Stainier, D.Y.R., 2001. Bmp2b and oep promote early myocardial differentiation through their regulation of gata5. Dev. Biol. 234 (2), 330–338. https://doi.org/10.1006/dbio.2001.0259.

Reppert, S.M., Weaver, D.R., 2001. Molecular analysis of mammalian circadian rhytms. Annu. Rev. Plant Physiol. Plant Mol. Biol. 63 (1), 647–676. https://doi.org/10.1146/annurev.arplant.52.1.139.

Roberts, A.P., Alloy, M.M., Oris, J.T., 2017. Review of the photo-induced toxicity of environmental contaminants. Comp. Biochem. Physiol., Part C: Toxicol. Pharmacol. 191, 160–167. https://doi.org/10.1016/j.cbpc.2016.10.005.

Robinson, M.D., Oshlack, A., 2010. A scaling normalization method for differential expression analysis of RNA-seq data. Genome Biol. 11 (3), 1–9. https://doi.org/10.1186/gb-2010-11-3-r25.

Ross, S.A., McCaffery, P.J., Drager, U.C., De Luca, L.M., 2000. Retinoids in embryonal development. Physiol. Rev. 80 (3), 1021–1054. https://doi.org/10.1152/physrev.2000.80.3.1021.

Sayed, A.E.-D.H., Mitani, H., 2016. The notochord curvature in medaka (Oryzias latipes) embryos as a response to ultraviolet a irradiation. J. Photochem. Photobiol. B Biol. 164, 132–140. https://doi.org/10.1016/j.jphotobiol.2016.09.023.

Schemeth, D., Nielsen, N.J., Andersson, J.T., Christensen, J.H., 2019. A tiered analytical approach for target, non-target and suspect screening analysis of polar transformation products of polycyclic aromatic compounds. Chemosphere 235, 175–184. https://doi.org/10.1016/j.chemosphere.2019.06.149.

Schlenk, D., Celander, M.C., Gallagher, E.P., George, S., James, M., Kullman, S.W., Willett, K., 2008. Biotransformation in fishes. In: Giulio, R.T. Di, Hinton, D.E. (Eds.), The Toxicology of Fishes. Taylor & Francis, Washington, DC, pp. 153–234.

Scott, J.A., Incardona, J.P., Pelkki, K., Shepardson, S., Hodson, P.V., 2011. AhR2-mediated, CYP1A-independent cardiovascular toxicity in zebrafish (Danio rerio) embryos exposed to retene. Aquat. Toxicol. https://doi.org/10.1016/j.aquatox.2010.09.016.

Senft, A.P., Dalton, T.P., Nebert, D.W., Genter, M.B., Puga, A., Hutchinson, R.J., Shertzer, H.G., 2002. Mitochondrial reactive oxygen production is dependent on the aromatic hydrocarbon receptor. Free Radic. Biol. Med. 33 (9), 1268–1278. https://doi.org/10.1016/S0891-5849(02)01014-6.

Serigstad, B., Adoff, G.R., 1985. Effects of oil exposure on oxygen consumption of cod eggs and larvae. Mar. Environ. Res. 17 (2–4), 266–268. https://doi.org/10.1016/0141-1136(85)90102-3.

Shin, S., Wakabayashi, N., Misra, V., Biswal, S., Lee, G.H., Agoston, E.S., Kensler, T.W., 2007. NRF2 modulates aryl hydrocarbon receptor signaling: influence on adipogenesis. Mol. Cell. Biol. 27 (20), 7188–7197. https://doi.org/10.1128/mcb.00915-07.

Simon, H.U., Haj-Yehia, A., Levi-Schaffer, F., 2000. Role of reactive oxygen species (ROS) in apoptosis induction. Apoptosis 5 (5), 415–418. https://doi.org/10.1023/A:1009616228304.

Sørensen, L., Meier, S., Mjøs, S.A., 2016. Application of gas chromatography/tandem mass spectrometry to determine a wide range of petrogenic alkylated polycyclic aromatic hydrocarbons in biotic samples. Rapid Commun. Mass Spectrom. 30 (18), 2052–2058. https://doi.org/10.1002/rcm.7688.

Sørensen, L., Silva, M.S., Booth, A.M., Meier, S., 2016. Optimization and comparison of miniaturized extraction techniques for PAHs from crude oil exposed Atlantic cod and haddock eggs. Anal. Bioanal. Chem. 408 (4), 1023–1032. https://doi.org/10.1007/s00216-015-9225-x.

Sørensen, L., Sørhus, E., Nordtug, T., Incardona, J.P., Linbo, T.L., Giovanetti, L., Meier, S., 2017. Oil droplet fouling and differential toxicokinetics of polycyclic aromatic hydrocarbons in embryos of Atlantic haddock and cod. PLoS One 12 (7), 1–26. https://doi.org/10.1371/journal.pone.0180048.

Sørensen, L., Hansen, B.H., Farkas, J., Donald, C.E., Robson, W.J., Tonkin, A., Rowland, S.J., 2019. Accumulation and toxicity of monoaromatic petroleum hydrocarbons in early life stages of cod and haddock. Environ. Pollut. 251, 212–220. https://doi.org/10.1016/j.envpol.2019.04.126.

Sørhus, E., Incardona, J.P., Karlsen, Ø., Linbo, T., Sørensen, L., Nordtug, T., Meier, S., 2016. Crude oil exposures reveal roles for intracellular calcium cycling in haddock craniofacial and cardiac development. Sci. Rep. 6 (31058), 1–21. https://doi.org/10.1038/srep31058.

Sørhus, E., Incardona, J.P., Furmanek, T., Goetz, G.W., Scholz, N.L., Meier, S., Jentoft, S., 2017. Novel adverse outcome pathways revealed by chemical genetics in a developing marine fish. elife 6, 1–30. https://doi.org/10.7554/elife.20707.

Sørhus, E., Donald, C.E., da Silva, D., Thorsen, A., Karlsen, Ø., Meier, S., 2021. Untangling mechanisms of crude oil toxicity: linking gene expression, morphology and PAHs at two developmental stages in a cold-water fish. Sci. Total Environ. 757, 143896. https://doi.org/10.1016/j.scitotenv.2020.143896.

Star, B., Nederbragt, A.J., Jentoft, S., Grimholt, U., Malmstrøm, M., Gregers, T.F., Jakobsen, K.S., 2011. The genome sequence of Atlantic cod reveals a unique immune system. Nature 477, 207–210. https://doi.org/10.1038/nature10342.

Stegeman, John J., Hahn, M.E., 1994. Biochemistry and molecular biology of monooxygenases: current perspectives on forms, functions, and regulation of cytochrome P450 in aquatic species. In: Malins, D.C., Ostrander, G.K. (Eds.), Aquatic Toxicology: Molecular, Biochemical and Cellular Perspectives. Taylor & Francis, Washington, DC, pp. 87–206.

Stegeman, J.J., Lech, J.J., 1991. Cytochrome P-450 monooxygenase systems in aquatic species: carcinogen metabolism and biomarkers for carcinogen and pollutant exposure. Environ. Health Perspect. 90, 101–109. https://doi.org/10.2307/3430851.

Stohs, S.J., 1990. Oxidative stress induced by 2,3,7,8-tetrachlorodibenzo-p-dioxin (TCDD). Free Radic. Biol. Med. 9, 79–90.

Sundell, K., Björnsson, B.T., 1990. Effects of vitamin D, 25 (OH) vitamin D, 24, 25 (0H), vitamin D, and 1, 25 (OH), vitamin D, on the in vitro intestinal calcium absorption in the marine teleost, Atlantic cod (Gadus morhua). Gen. Comp. Endocrinol. 78, 74–79.

Sundell, K., Norman, A.W., Björnsson, B.T., 1993. 1,25(OH)2 vitamin D3 increases ionized plasma calcium concentrations in the immature Atlantic cod Gadus morhua. Gen. Comp. Endocrinol. 91, 344–351.

Sundt, R.C., Ruus, A., Jonsson, H., Skarphédinsdóttir, H., Meier, S., Grung, M., Pampanin, D.M., 2012. Biomarker responses in Atlantic cod (Gadus morhua) exposed to produced water from a North Sea oil field: laboratory and field assessments. Mar. Pollut. Bull. 64 (1), 144–152. https://doi.org/10.1016/j.marpolbul.2011.10.005.

Swartz, M.E., Sheehan-Rooney, K., Dixon, M.J., Eberhart, J.K., 2011. Examination of a palatogenic gene program in zebrafish. Dev. Dyn. 240 (9), 2204–2220. https://doi.org/10.1002/dvdy.22713.

Szklarczyk, D., Gable, A.L., Lyon, D., Junge, A., Wyder, S., Huerta-Cepas, J., Von Mering, C., 2019. STRING v11: protein-protein association networks with increased coverage, supporting functional discovery in genome-wide experimental datasets. Nucleic Acids Res. 47 (D1), D607–D613. https://doi.org/10.1093/nar/gky1131.

Tappenden, D.M., Lynn, S.G., Crawford, R.B., Lee, K.A., Vengellur, A., Kaminski, N.E., LaPres, J.J., 2011. The aryl hydrocarbon receptor interacts with ATP5α1, a subunit of the ATP synthase complex, and modulates mitochondrial function. Toxicol. Appl. Pharmacol. 254 (3), 299–310. https://doi.org/10.1016/j.taap.2011.05.004.

Tilseth, S., Solberg, T.S., Westrheim, K., 1984. Sublethal effects of the water-soluble fraction of ekofisk crude oil on the early larval stages of cod (Gadus morhua L.). Mar. Environ. Res. 11 (1), 1–16. https://doi.org/10.1016/0141-1136(84)90007-2.

Torres Nuñez, E., Sobrino, C., Neale, P.J., Ceinos, R.M., Du, S., Rotllant, J., 2012. Molecular response to ultraviolet radiation exposure in fish embryos: implications for survival and morphological development. Photochem. Photobiol. 88 (3), 701–707. https://doi.org/10.1111/j.1751-1097.2012.01088.x.

Tseng, H.P., Hseu, T.H., Buhler, D.R., Wang, W.Der, Hu, C.H., 2005. Constitutive and xenobiotics-induced expression of a novel CYP3A gene from zebrafish larva. Toxicol. Appl. Pharmacol. 205 (3), 247–258. https://doi.org/10.1016/j.taap.2004.10.019.

Van Tiem, L.A., Di Giulio, R.T., 2011. AHR2 knockdown prevents PAH-mediated cardiac toxicity and XRE- and ARE-associated gene induction in zebrafish (Danio rerio). Toxicol. Appl. Pharmacol. 254, 280–287. https://doi.org/10.1016/j.taap.2011.05.002.

Vandesompele, J., De Preter, K., Pattyn, F., Poppe, B., Van Roy, N., De Paepe, A., Speleman, F., 2002. Accurate normalization of real-time quantitative RT-PCR data by geometric averaging of multiple internal control genes. Rock Mech. Rock. Eng. 3 (7), 1–12. https://doi.org/10.1007/s00603-018-1496-z.

Wang, L., Gallagher, E.P., 2013. Role of Nrf2 antioxidant defense in mitigating cadmium-induced oxidative stress in the olfactory system of zebrafish. Toxicol. Appl. Pharmacol. 266 (2), 177–186. https://doi.org/10.1016/j.taap.2012.11.010.

Weger, B.D., Sahinbas, M., Otto, G.W., Mracek, P., Armant, O., Dolle, D., Dickmeis, T., 2011. The light responsive transcriptome of the zebrafish: function and regulation. PLoS One 6 (2). https://doi.org/10.1371/journal.pone.0017080.

Wernersson, A.S., 2003. Predicting petroleum phototoxicity. Ecotoxicol. Environ. Saf. 54 (3), 355–365. https://doi.org/10.1016/S0147-6513(02)00083-0.

Whitlock, J.P.J., 1999. Induction of cytochrome P4501a1. Annu. Rev. Pharmacol. Toxicol. 39 (1), 103–125. https://doi.org/10.1146/annurev.pharmtox.39.1.103.

Wincent, E., Jönsson, M.E., Bottai, M., Lundstedt, S., Dreij, K., 2015. Aryl hydrocarbon receptor activation and developmental toxicity in zebrafish in response to soil extracts containing unsubstituted and oxygenated pahs. Environ. Sci. Technol. 49 (6), 3869–3877. https://doi.org/10.1021/es505588s.

Wincent, E., Le Bihanic, F., Dreij, K., 2016. Induction and inhibition of human cytochrome P4501 by oxygenated polyciyclic aromatic hydrocarbons. Toxicol. Res. 5, 788–799.

Xu, W., Barrientos, T., Andrews, N.C., 2013. Iron and copper in mitochondrial diseases. Cell Metab. 17 (3), 319–328. https://doi.org/10.1038/jid.2014.371.

Yadetie, F., Zhang, X., Hanna, E.M., Aranguren-Abadía, L., Eide, M., Blaser, N., Karlsen, O.A., 2018. RNA-seq analysis of transcriptome responses in Atlantic cod (Gadus morhua) precision-cut liver slices exposed to benzo[a]pyrene and 17A-ethynylestradiol. Aquat. Toxicol. 201, 174–186. https://doi.org/10.1016/j.aquatox.2018.06.003.

Yang, W.S., Stockwell, B.R., 2016. Ferroptosis: death by lipid peroxidation. Trends Cell Biol. 26 (3), 165–176. https://doi.org/10.1016/j.tcb.2015.10.014.

Yeager, R.L., Reisman, S.A., Aleksunes, L.M., Klaassen, C.D., 2009. Introducing the "TCDD-inducible AhR-Nrf2 gene battery". Toxicol. Sci. 111 (2), 238–246. https://doi.org/10.1093/toxsci/kfp115.

Yelon, D., Horne, S.A., Stainier, D.Y.R., 1999. Restricted expression of cardiac myosin genes reveals regulated aspects of heart tube assembly in zebrafish. Dev. Biol. 214 (1), 23–37. https://doi.org/10.1006/dbio.1999.9406.

Yin, J.-J., Xia, Q., Cherng, S.-H., Tang, I.-W., Fu, P.P., Lin, G., Yu, H., Sáenz, D.H., 2008. UVA photoirradiation of oxygenated benz[a]anthracene and 3-methylcholanthene - generation of singlet oxygen and induction of lipid peroxidation. Int. J. Environ. Res. Public Health 5 (1), 26–31. https://doi.org/10.3390/ijerph5010026.

Yu, H., 2002. Environmental carcinogenic polycyclic aromatic hydrocarbons: photochemistry and phototoxicity. J. Environ. Sci. Health C Environ. Carcinog. Ecotoxicol. Rev. 20 (2), 149–183. https://doi.org/10.1081/GNC-120016203.

Zagarese, H.E., Williamson, C.E., 2001. The implications of solar UV radiation exposure for fish and fisheries. Fish Fish. 2 (3), 250–260. https://doi.org/10.1046/j.1467-2960.2001.00048.x.

Zhang, X., Jonassen, I., 2020. RASflow: an RNA-seq analysis workflow with snakemake. BMC Bioinf. 21 (110), 1–9. https://doi.org/10.1101/839191.

Zhao, X., Ren, X., Zhu, R., Luo, Z., Ren, B., 2016. Zinc oxide nanoparticles induce oxidative DNA damage and ROS-triggered mitochondria-mediated apoptosis in zebrafish embryos. Aquat. Toxicol. 180, 56–70. https://doi.org/10.1016/j.aquatox.2016.09.013.

Zhou, Y., Zhou, B., Pache, L., Chang, M., Khodabakhshi, A.H., Tanaseichuk, O., Chanda, S.K., 2019. Metascape provides a biologist-oriented resource for the analysis of systems-level datasets. Nat. Commun. 10 (1). https://doi.org/10.1038/s41467-019-09234-6.